ISSN 1831-9424

European Commission

JRC TECHNICAL REPORT

Report on new Pléiades Neo sensors benchmark

Geometric benchmarking over Maussane test site for CAP 2014+ purposes

Loudjani, P., Lemajic, S., .Parage, V., Rodrigues, C.

2023

Joint Research Centre

EUR 31687 EN

Contact information
Name: Philippe Loudjani
Address: Joint Research Centre, Via Enrico Fermi 2749, TP 272, 21027 Ispra (VA), Italy
Email: philippe.loudjani@ec.europa.eu
Tel.: 39 0332 78 6160

EU Science Hub
https://joint-research-centre.ec.europa.eu

JRC134704

EUR 31687 EN

PDF ISBN 978-92-68-08187-7 ISSN 1831-9424 doi:10.2760/38474 KJ-NA-31-687-EN-N

Ispra: European Commission, 2023

How to cite this report: Loudjani P., .Lemajic S., Parage V., and Rodrigues C., *Report on new Pléiades Neo sensors benchmark*, European Commission, Ispra, 2023, doi:10.2760/38474, JRC134704.

Contents

Abstract ... 1

Executive summary ... 2

1 Introduction ... 3

2 Pléiades Neo satellite ... 4

3 Pléiades Neo image products (information provided by Airbus) ... 6

3.1 Spectral Band Combinations ... 6

3.2 Geometric Processing Levels ... 7

4 Study Area ... 9

5 Auxiliary data and imagery used ... 10

5.1 Ground Control Points ... 10

5.2 Digital Elevation Model (DEM) ... 14

5.3 Aerial Orthomosaics used ... 15

5.4 Pléiades Neo satellite imagery used ... 15

5.5 Software ... 17

6 Pléiades Neo Benchmarking Tests ... 19

6.1 Benchmarking Methodology ... 19

6.2 Test Scenarios ... 19

6.3 Internal Quality Control (Airbus) ... 21

7 External Quality Control ... 26

7.1 Method for external quality check (EQC) of ortho imagery ... 26

7.1.1 Independent check points (ICPs) selection and distribution ... 26

7.1.2 Geometric quality assessment-measurements and calculations ... 28

8 Results and discussions ... 30

8.1 Impact of the orthorectification model ... 30

8.2 Impact on the number of GCPs used for the image processing ... 33

8.3 Impact of software used ... 36

8.4 Impact of image acquisition angles ... 37

8.5 Impact of Pleaides sensors ... 39

8.6 Summarising values ... 39

9 Conclusions ... 41

References ... 42

List of abbreviations and definitions ... 43

List of figures ... 44

List of tables ... 46

Abstract

In order to be used in the frame of the Common Agricultural Policy (CAP) 2014+ direct payments' management, all Very High Resolution (VHR) imagery should comply with spatial accuracy compatible with a scale of 1:5000 or larger. To check this, the JRC has set a benchmarking test to verify whether the planimetric accuracy of produced ortho imagery of any new VHR sensor does not exceed certain thresholds.

The JRC has been contacted by Airbus Defence and Space Intelligence Company to test their new Pléiades Neo VHR sensors. The benchmarking tests were carried out on six Pléiades Neo 3 and 4 imagery collected between February and May 2022. This report describes in detail how the tests were performed i.e. auxiliary data used, methodology and workflow as well as outcome from the Internal Quality Control. Tests are performed by the sensor Company itself but, to make the tests objective, the JRC also performs an external Quality Control which is a base for certification of the sensor.

The results of these tests allowed to conclude that the imagery collected by recently launched Pléiades NEO satellites can be potentially used in the frame of The CAP 2014+ image acquisition campaign. This conclusion remains valid under certain conditions of image acquisition angles and ortho rectification process.

(To note that the benchmarking tests have been set for the CAP 2014+ technical specifications and were valid until 31 December 2022. For the CAP 2023+, entering into force on 1st January 2023, new technical specifications will be set to comply with the new VHR imagery use requirements i.e. in the frame of Quality Assessment processes).

Authors

Loudjani P. (European Commission, Joint Research Centre (JRC), Ispra, Italy), Lemajic S. (Fincons SpA, Milan, Italy), Parage V., and Rodrigues C. (Airbus Defence and Space Intelligence, Toulouse, France)

Executive summary

The main objective of the present report is to assess whether the new Very High Resolution (VHR) Pléiades Neo sensors can be qualified for Control with Remote Sensing (CwRS) programme, in Common Agriculture Policy (CAP). The benchmarking presented herein aims at evaluating the usability of Pléiades Neo for the CAP checks through an estimation of its geometric (positional) accuracy, as well as measuring the influence of different factors (viewing angle, number of GCPs, software implementation) on this accuracy. For that purpose, apart from checking the results of the Internal Quality Control of Airbus Company, an independent External Quality Control is done to verify if the orthoimagery conforms to the standard method developed by JRC.

Benchmarking tests were carried out on 6 images acquired over an Area of Interest (AOI) close to Maussane (France). For the two sensors (Pléiades Neo 3 and 4) 3 images have been acquired, between February and May 2022, with three configurations of acquisition to test the orthorectification process.

This report describes in detail how the tests were performed i.e. auxiliary data used (chapter 5), methodology and workflow (chapter 6).

The outcome from the Internal Quality Control performed by Airbus are given in chapter 6.3. The details of the independent External Quality Control handled by JRC are provided in Chapter 7 while the results are detailed in Chapter 8.

In the light of the benchmark tests performed on Pléiades NEO ortho products, one can draw the conclusion that the Neo ortho imagery geometric accuracy potentially meets the requirements of RMSEx ≤1.25m and RMSEy ≤1.25 for the VHR prime profiles defined in the VHR profile based technical specifications.

These results were obtained for tests with imagery acquired with 5˚, 20˚ and 30˚ Off Nadir Angles (ONA), with at least 3 GCPs use for orthorectification and with RPC or rigorous models.

It must be noted that when rectification were made without GCPs, results obtained become out of specifications for acquisitions 30˚ ONA and even 20˚ in some case for Pléiades Neo4 sensor.

The reservation made on fully meeting the requirements lies on the fact that, sometimes, atypical results were obtained such as higher RMSE observed for near nadir acquisition compared to 20˚ or 30˚ ONA. However, the number of images made available was insufficient to further investigate this phenomenon.

To note also, that at the time of the benchmark analysis, Airbus production chain was not yet fully finalised and internal references were not yet implemented. Airbus recently informed us that, according to the tests they performed using internal references that will be implemented soon in its production chain, the results are within the specifications whatever the PNEO sensor for angles up to 30° ONA. This should be further confirmed but the JRC benchmarking work was already concluded at the time of this notification.

Finally, one should remind that the available JRC's GCPs dataset is now dating. Several points became unreliable since changes occurred on the ground. Even if these points were generally discarded, one can argue that RMSEs estimated may hold some uncertainty.

Policy context

The benchmarking tests were set to be used in the frame of the Common Agricultural Policy (CAP) 2014+ direct payments' management. The aim was to verify that all used Very High Resolution (VHR) imagery would comply with spatial accuracy compatible with a scale of 1:5000 or larger.

The benchmarking tests were performed by JRC, under an Administrative Arrangement with DG Agriculture, and upon request of image providers proposing new VHR sensors. This Benchmarking activity has thus ceased on the 31st December 2022 with the ending of the CAP2014+.

For the CAP 2023+, new technical specifications will be set to comply with the new VHR imagery use requirements i.e. in the frame of Quality Assessment processes. Should sensor benchmarking tests be put in place, they would need to be done according to these up-dated technical specifications.

1 Introduction

This report describes in details steps that have been taken to check if Pléiades Neo sensors qualify for the Common Agricultural Policy (CAP) image acquisition Campaign. The main requirement according to VHR image acquisition specifications for the CAP 2014+ checks [ii] is to have a spatial resolution compliant with at least a scale of 1:5000 or larger. This translates into a required the planimetric accuracy of:

- RMSEx ≤1.25m and RMSEy ≤1.25 for VHR Prime
- RMSEx ≤5m and RMSEy ≤5m for VHR Backup

Several scenarios are built to test the possible influence of different factors on the ortho imagery accuracy, i.e.:

- number and distribution of Ground Control Points (GCPs);
- incidence angle;
- and the sensor model implemented in the software (ENVI and ERDAS).

2 Pléiades Neo satellite

From the information provided by Airbus Defence and Space Intelligence Company (later on in the text called Airbus), Pléiades Neo is a constellation of potentially four identical, very high-resolution optical satellites. 2 were launched in 2021 and 2 others to be launched in late 2022 on board Arianespace's Vega rocket but the launch failed. With a 10-year expected lifetime, they will ensure the provision of 30cm resolution imagery until at least 2032, and consequently the continuity of Airbus Intelligence's high standard geo-information services.

Table 1. General characteristics of the Pléiades Neo constellation

Number of satellites	Four identical satellites in constellation, named: • Pléiades Neo 3 • Pléiades Neo 4 • Pléiades Neo 5 (not available) • Pléiades Neo 6 (Not available)
Launch mass Launch	Body: ~1 ton for each satellite 2021 for Pléiades Neo 3 & 4 2022 for Pléiades Neo 5 & 6 (launch failed)
Mission lifetime	10 years for each satellite

Source: Airbus

Pléiades Neo operates as a genuine constellation on the same orbit and phased 90° from each other. Added to their oblique incidence capability (up to 52° angle) and exceptional agility, this orbit phasing allows the satellites to visit any point on the globe twice daily – ideal for monitoring sensitive sites, anticipating risks, effectively managing crises and for coverage of large areas.

Table 2. Orbital characteristics and viewing capability

Orbit Altitude Cycle	Sun-synchronous, 10:30 a.m. descending node 620km 26 days
Period/Inclination	97.2°/97.9°
Frequency of visit (with four satellites)	Twice a day, anywhere
Acquisition capability	Up to 2 million km² per day (*with four satellites*)
Nominal imaging mode	14km-swath strips oriented along North-South axis
Stereo capability	Single-pass stereo and tri-stereo (fore., nadir and aft. mode)

Source: Airbus

The twice-daily visit capacity is backed by a very reactive operational loop. Work plans are updated every 25 minutes and pooled: when an image is to be collected by one satellite, the related acquisition request is removed from the tasking plans of the other satellites. These multiple and synchronised daily work plans enable easy handling of last-minute tasking requests, as well as integration of the latest weather information for an improved data collection success rate.

In addition, Airbus's network of ground receiving stations enable an all-orbit contact and ensure near real-time performances worldwide and rapid data-access, to deliver the highest standards in our service response times. Images are downlinked at each orbit, automatically processed and quickly delivered to the customer, allowing faster results in emergency situations.

For the user, this results in:

- More image collection opportunities.
- Improved map update capacity (coverage).
- Rapid access to data after acquisition.
- Unprecedented capacity for disaster response, regular or intensive monitoring, or change detection.

Table 3. Key attributes of the Pléiades Neo Constellation

Main X-band receiving stations S-band uplink stations	Toulouse (France) Kiruna (Sweden) Inuvik (Canada) Kiruna (Sweden) Inuvik (Canada)
Programming centre	Airbus/Geo-Intelligence – Toulouse (France) Airbus/Geo-Intelligence – Chantilly VA (USA)
Production centre	Airbus DS Intelligence – Toulouse (France)
Tasking plans refresh frequency	Every orbit: 15 times/day/satellite (60 times a day in total)
Update of weather forecast Satellite Control Centre	4 times a day for global weather forecast + at each orbit: weather update for the next 2 hours Toulouse (France)

Source: Airbus

As advertised by Airbus, the Pléiades Neo satellites benefit from exceptional performance in terms of agility (roll/pitch: 10° in 7 seconds, 30° in 12 seconds, 60° in 20 seconds). The time required to slew 200 kilometres (17°) is reduced to 10 seconds, including stabilisation time. This kind of performance results in a reduced average acquisition window for the users, allowing more images to be collected during the same pass. Collection opportunities are more numerous, conflicts between contiguous requests are minimised, and the acquisition on the same pass of either big Area of Interests (AOIs) or several targets at the same latitude is improved.

The Pléiades Neo constellation offers a wide range of products and services featuring different options to match as closely as possible to any customer requirements. Combining the Panchromatic and multispectral bands, images can be visualised as either black and white (30 cm product resolution), natural colours, false colours (1.2m product resolution) or as merged product (Pan-sharpened colour image) with the resolution of a Panchromatic image.

3 Pléiades Neo image products (information provided by Airbus)

3.1 Spectral Band Combinations

Pléiades Neo delivers ready-to-use products, which can be easily integrated in GIS and/or transformed into thematic information when combined with other satellite, airborne or ground information. Pléiades Neo satellites always acquire images simultaneously in two modes:

- **Panchromatic**: one band (black and white with 30 cm product resolution)
- **Multispectral**: six bands (colour with 1.2m product resolution)

Compared to Pléiades satellites generation, Pléiades Neo has two additional multispectral bands:

- **Deep-blue:** allows deeper penetration into water bodies, and is very useful in bathymetric studies, and has better characterisation of atmospheric conditions and discrimination in shadows.
- **Red-edge:** is particularly useful for agricultural and vegetation-related applications as it provides crop and vegetation status through photosynthesis characterisation. Once canopy closure is reached (NDVI is saturating), Red-edge can differentiate between the various densities of canopy.

The Multispectral products are offered as four or six-band products:

- **MS:** Multispectral (4 bands RGB+NIR)
- **Full MS:** Multispectral (6 bands RGB+NIR+ Deep-blue + Red-edge)

Panchromatic and Multispectral image products are co-registered (completely superimposable).

Pan-sharpened Products:
Pan-sharpened Products are the products provided for the different test of this benchmark.
Pan-sharpened products combine the visual coloured information of the Multispectral data with the details provided by the panchromatic data, resulting in a higher resolution 0.3m colour product.
Typically, three or four low-resolution visible bands – blue, green and red or green, red and near infrared – are used as the main inputs in the process to produce a very high-resolution natural colour or false colour image.
For Pan-sharpened products, Airbus uses its proprietary fusion processing. Performing its own pan-sharpening is a fine process.
Pan-sharpened products are offered as three, four and six-band products:

- PMS_N: Pansharpening in natural colour (3 bands RGB)
- PMS_X: Pansharpening in false colour (3 bands NIRRG)
- PMS: Pansharpening (4 bands RGB+NIR)
- Full PMS: Pansharpening (6 bands)
- The Pléiades Neo constellation offers a wide range of products and services featuring different options to match as closely as possible to any customer requirements.

Table 4. Standard product options delivered by Image Production Facility

Geometric processing options	Primary Projected Ortho
Radiometric processing options	Basic Reflectance Display
Imagery format	JPEG 2000 Optimised JPEG 2000 Regular GeoTIFF
Product encoding	12 bits 8 bits
Spectral combinations	PAN: Panchromatic (1 band) Bundle: PAN + MS (4 bands RGB+NIR) Full Bundle: PAN + Full MS (6 bands) MS: Multispectral (4 bands RGB+NIR) Full MS: Multispectral (6 bands) PMS_N: Pansharpening in natural colour (3 bands RGB) PMS_X: Pansharpening in false colour (3 bands RGNIR) PMS: Pansharpening (4 bands RGB+NIR) Full PMS: Pansharpening (6 bands)

Source: Airbus

3.2 Geometric Processing Levels

Pléiades Neo core imagery products are available in three different geometric processing levels: Primary, Projected and Ortho.

All Pléiades Neo products are corrected for non-uniformity sensor radiometric and distortions, using internal calibration parameters, ephemeris and attitude measurements.

Standard products offer the Panchromatic channel (product resolution: 0.3m) or the Multispectral channels (six bands, product resolution: 1.2m) already registered and possibly merged.

Primary products:

This Primary product corresponds to that of the products supplied as input by Airbus in order to carry out the various orthorectification tests of this Benchmark.

The Primary product is the geometric processing level closest to the source image acquired by the sensor. This product restores perfect collection conditions: the sensor is placed in rectilinear geometry, and the image is cleared of all radiometric distortion. This product is optimal for those clients familiar with satellite imagery processing techniques who want to apply their own production methods (orthorectification or 3D modelling for example). To this end, Rational Polynomial Coefficients (RPCs) and the sensor model are provided with the product to ensure full autonomy and simplicity for users. The Primary level product is:

- In sensor geometry, synthesised on a perfect single and linear push-broom array.
- With an equalised radiometry on the native dynamic range of the sensor, 12 bits (4096 values).

The product is extracted from one strip acquisition. The support for this extraction is a polygonal region of interest in WGS84 coordinates.

The main geometric processing includes:

The combination of all sub-swaths across the field of view (14km nadir condition): synthesis in a virtual focal plane represented by a single linear array for all spectral bands.

Correction of instrumental and optical distortions: viewing angles adjusted to the single linear array model.

Co-registration of all spectral bands: Multispectral and Panchromatic.

Attitudes and ephemeris data are refined at ground on the mean estimation:

- Adjustment of the time stamp sampling (along scan line).
- Attitudes filtering over time of acquisition.

Consistent alignment of the physical location model ancillary data and RPC analytic model data.

When appropriate the image location can be improved by Ground Control Points from the Airbus Intelligence worldwide Space Reference Points database.

The main radiometric corrections/enhancements include:

Inter-detector equalisation: correction of differences in sensitivity between the detectors (on-board correction).

Aberrant detectors correction (none at that time).

Panchromatic band restored and de-noised.

Orthoimages:

The description of the orthorectification process below concerns the 9 tests performed on orthorectified (Ortho) products from standard Airbus lines.

The Ortho product is a georeferenced image in Earth geometry, corrected from acquisition and terrain off-nadir effects. The Ortho is produced as a standard, with fully automatic processing.

The standard Ortho product is an image that has been corrected (viewing angle and ground effects) so that it can be superimposed on a map. In addition to radiometric and geometric adjustments, a geometric process using a relief model (known as orthorectification) eliminates the perspective effect on the ground (not on buildings), restoring the geometry of a vertical shot. The Ortho product is optimal for simple and direct use of the image. It can be used and ingested directly into a Geographic Information System.

This processing level facilitates the management of several layers of products, from the same sensor or others, while reducing localisation gaps that can be caused by different viewing angles or relief between the various layers. To improve the accuracy of the product, Airbus uses its own worldwide 3D reference layers to perform ground corrections: Space Reference Point Ground Control Points (GCP) and WorldDEM4Ortho hybrid DTM/DSM for orthorectification.

The product is extracted from one to several contiguous strip acquisitions: single ortho or mosaic. Support for this extraction is a polygonal region of interest in WGS84 coordinates.

The Ortho level product inherits the same geometric corrections from the Primary level, with additional adjustments:

Planimetric reset: On request, if ground reference data is available, the location is reset on Ground. By default, Space Reference Points are used, otherwise PAS ortho tiles are used where available.

Altimetric reset: with a Digital Elevation Model (DEM) to correct acquisition angles and relief off-nadir effects (as a vertical shot) for the ortho-rectification resampling process. By default, the WorldDEM4Ortho layer is used where available, otherwise Reference3D DEM or Shuttle Radar Topography Mission (SRTM) DEM is used.

Map projection or geographic projection.

The Ortho product inherits same radiometric corrections and enhancements from the Primary or Projected processing level, with additional adjustments:

Pixel sampling (Spline kernel) at a regular resolution of 1.2m for Multispectral products and 0.3m for Panchromatic and Pan-sharpened products.

4 Study Area

The test AOI is located in the commune Maussane-les-Alpilles in the Provence-Alpes-Cote d'Azur Region in southern France and is being used as a 'test site' by the European Commission since 1997. The AOI is characterized by different land use types and the terrain variations (high difference between highest and lowest point is around 300m). The area used in the tests is 100km2 and spans 4◦41' to 4◦48'E and 43◦40' to 43◦45'N (***Figure 1***)

Figure 1. Location of the test site and its AOI

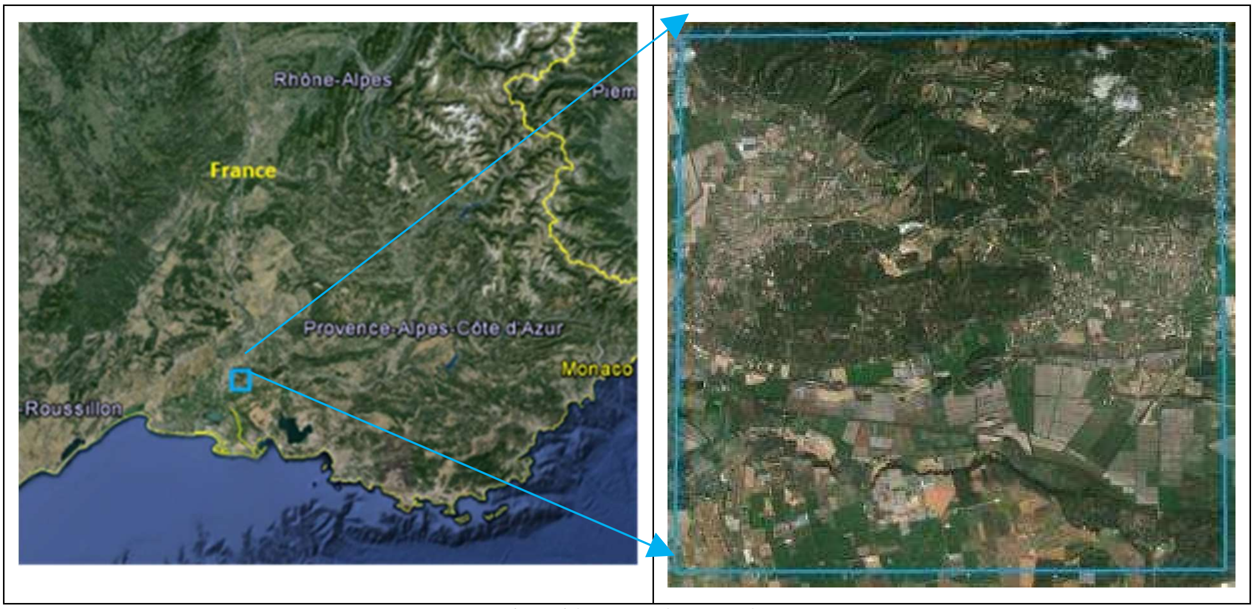

Source: JRC adapted from Google map information

5 Auxiliary data and imagery used

5.1 Ground Control Points

Ground Control Points play an important role in orthorectification process of satellite imagery aiming at improving the planimetric accuracy of created ortho images. These points cannot be randomly selected and the general principles for GCPs' selection would be as follows:

- should represent a prominent feature;
- should be well identified features;
- should be well identified in the image;
- should be well distributed;
- and objects that represent vertical displacements should not be used.

In addition, Guidelines for Best Practice and Quality Checking of Ortho Imagery [i] specifies the accuracy requirements for GCPs i.e.

''GCPs should be at least 3 times (5 times recommended) more precise than the target specification for the ortho, e.g. in the case of a target 2.5m RMSE, the GCPs should have a specification of 0.8m RMSE or better''.

According to VHR Image Acquisition Specifications for the CAP checks (CwRS and LPISQA) - VHR profile-based, target ortho image accuracy for VHR prime is 2m/1.5m/1.25m and 5m for VHR Backup [ii].

Considering all the above, set of 9 GCPs (***Table 5***, **Figure 2**) to be used in the modelling phase in the orthorectification process of six Pléiades NEO imageries has been selected from GCP dataset received from JRC.

Table 5. Ground Control Points available for the Maussane test site

Dataset	Point ID	RMSEx [m]	RMSEy [m]
ADS40_GCP_dataset_Maussane_ prepared_for_ADS40_in_2003	11XXXX	0,05	0,10
VEXCEL_GCP_dataset_Maussane_ prepared_for_VEXEL_in_2005	44XXXX	0,49	0,50
Multi-use_GCP_dataset_Maussane_ prepared_for_multi-use_in_Oct-2009	66XXX	0,30	0,30
Cartosat-1_GCP_dataset_Maussane_prepared_ for_Cartosat_in_2006	33XXX	0,55	0,37
Formosat-2_GCP_dataset_Maussane_ prepared_for_Formosat2_in_2007	7XXX	0,88	0,72
Cartosat-2_GCP_dataset_Maussane_ prepared_for_Cartosat-2_in_2009	55XXX	0,90	0,76
SPOT_GCP_dataset_Maussane_ prepared_for_SPOT_in_	22XXX	n/a	n/a
Maussane GNSS field campaign 21-26 November 2012	CXRX	0,15	0,15

Source: JRC

The GCPs were chosen from a set of existing collections of some 55 points in the area covering the Maussane site.

Figure 2. Distribution of GCPs available in the AOI, the background image is an elevation map of the area.

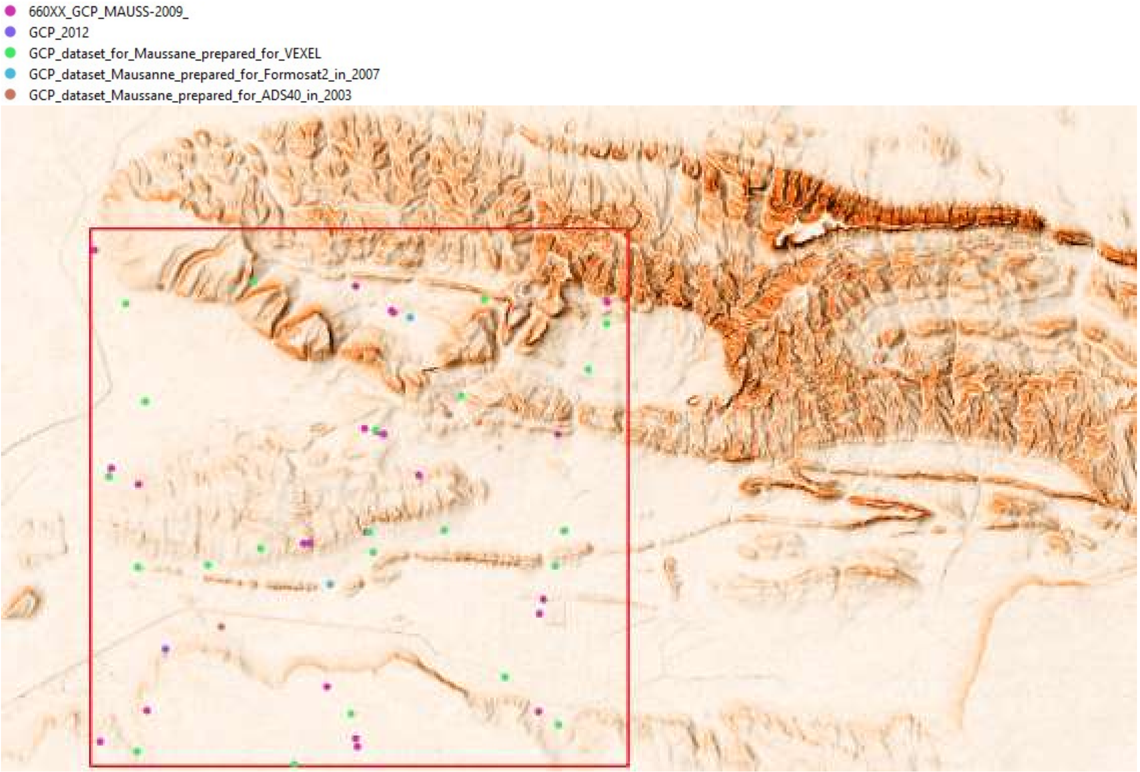

Source: JRC

GCPs Selection for orthorectification

A first selection of 9 GCPs was made in order to orthorectify the primary images according to the parameters provided in the different tests.

3 dataset have been used for this selection, 5 GCPs in MAUSS-2009, 3 GCPs for the dataset VEXEL and d 1 GCP selected in the dataset ADS40. The worst accuracy is 0.49m RMSE in x and 0.5m RMSE in y but still meeting the required specification. "GCPs [and ICPs] should be at least 3 times (5 times recommended) more precise than the target specification for the ortho, e.g. in the case of a target RSME1D _ 2:5m, the GCPs [and ICPs] should have a specification of RSME1D <= 0:8m."

Table 6. Collection used for the 9 GCPs selected for the orthorectification process

Dataset	Point ID	RMSEx [m]	RMSEy [m]	Number of GCPS selected
ADS40_GCP_dataset_Maussane_ prepared_for_ADS40_in_2003	11XXXX	0,05	0,10	1
VEXCEL_GCP_dataset_Maussane_ prepared_for_VEXEL_in_2005	44XXXX	0,49	0,50	3
Multi-use_GCP_dataset_Maussane_ prepared_for_multi-use_in_Oct-2009	66XXX	0,30	0,30	5

Source: JRC

Figure 3. Distribution of 9 GCPs selected for orthorectification process, the background image represents an elevation map of the area and the red square corresponding to the study AOI.

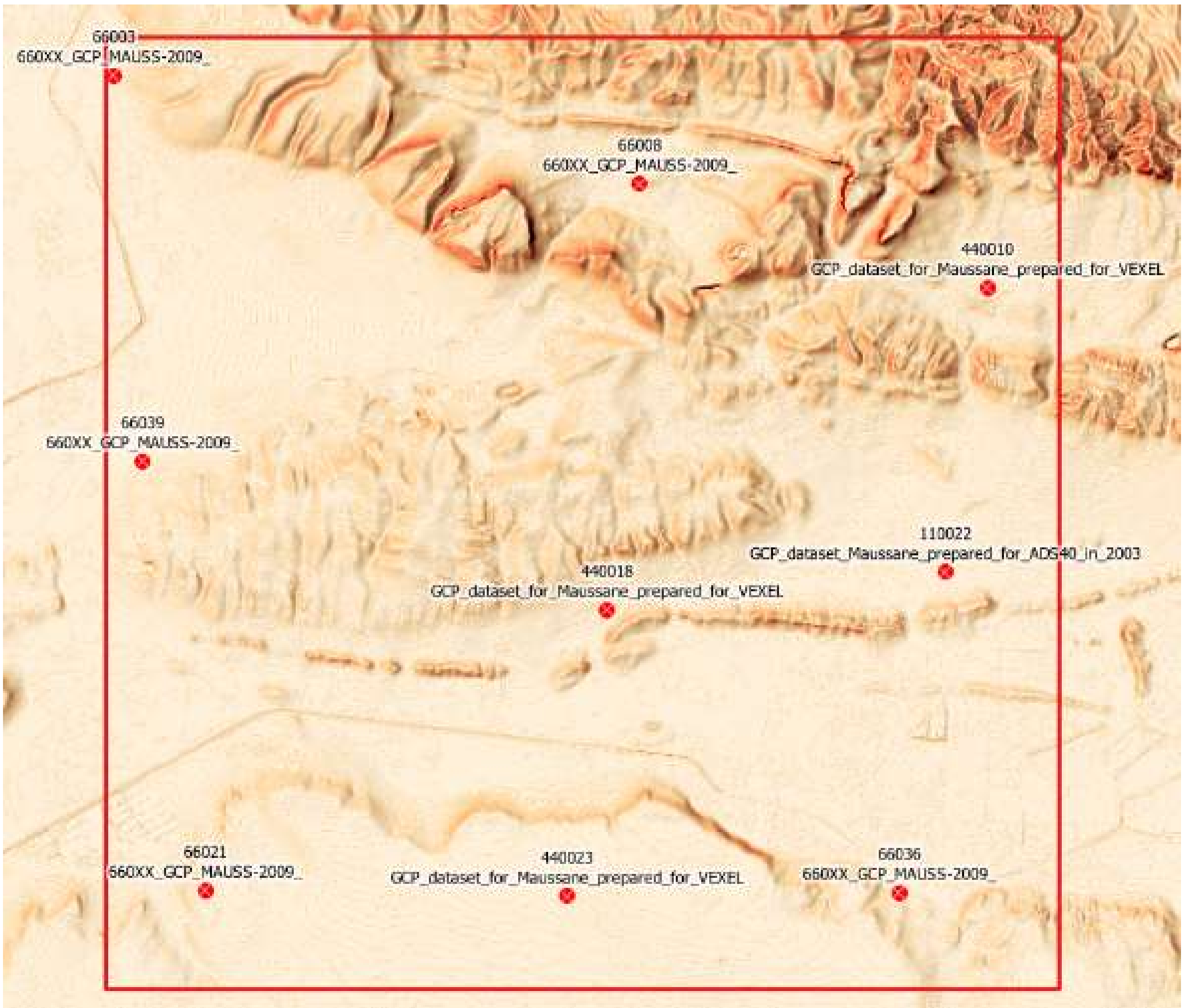

Source: JRC

<u>GCPs Selection for internal control</u>

Another set of 9 control points has been selected allowing independent internal control of the orthoimages to ensure their quality.

2 dataset have been used for this selection 4 GCPs in MAUSS-2009 and 5 GCPs for the dataset VEXEL. Like for the first selection the worst accuracy is 0.49m RMSE in x and 0.5m RMSE in y. These accuracies are meeting the required specifications.

Table 7. Collection used for the 9 GCPs selected for the internal control

Dataset	Point ID	RMSEx [m]	RMSEy [m]	Number of GCPS selected
VEXCEL_GCP_dataset_Maussane_ prepared_for_VEXEL_in_2005	44XXXX	0,49	0,50	5
Multi-use_GCP_dataset_Maussane_ prepared_for_multi-use_in_Oct-2009	66XXX	0,30	0,30	4

Source: JRC

Figure 4. Distribution of 9 GCPs selected for internal control, the background image represents an elevation map of the area and the red square corresponding to the study AOI

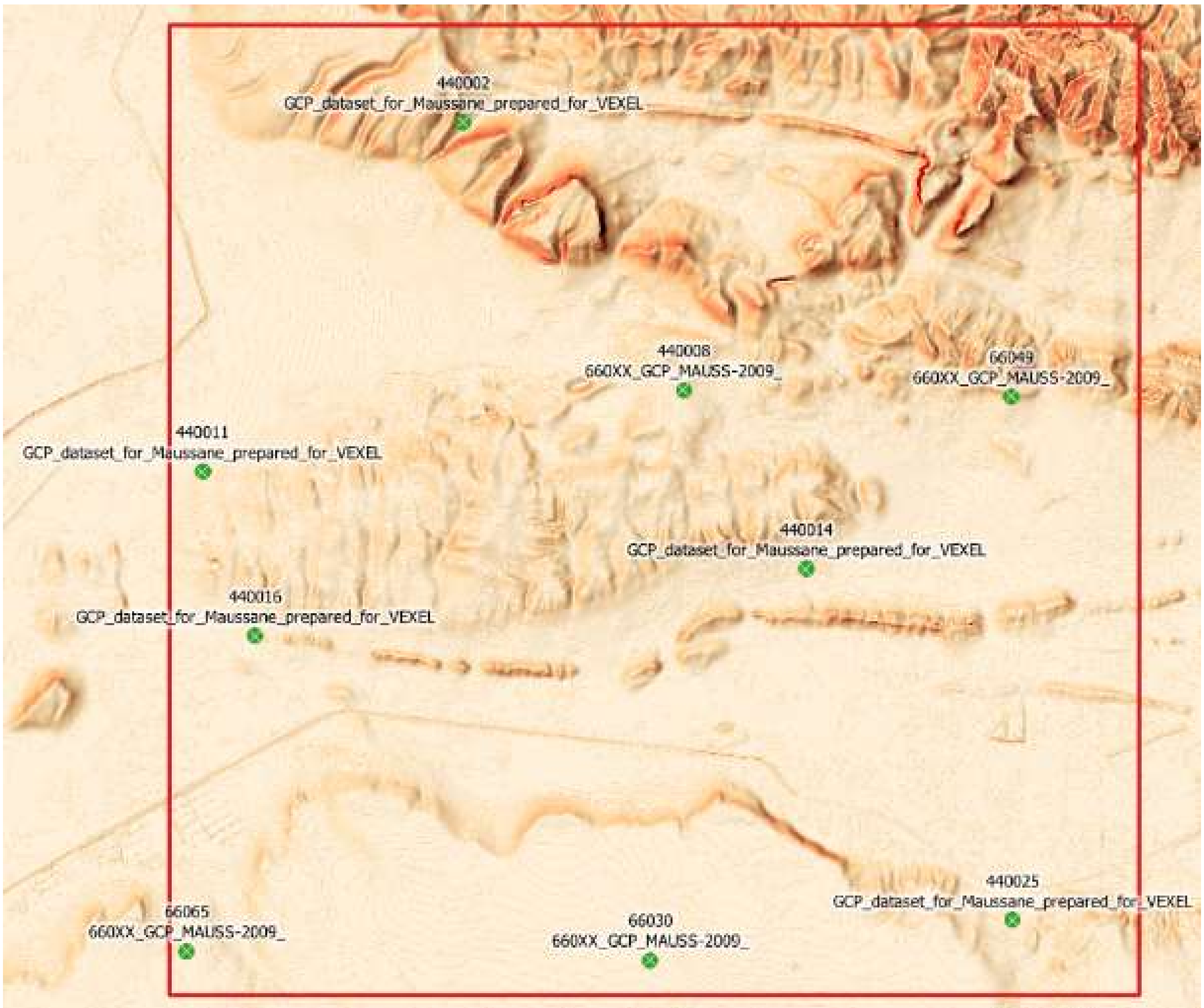

Source: JRC

The selection of GCPs was done to ensure a good distribution of points over the entire area trying to follow the model of the 3 _ 3 spatial pattern of von Gruber points (like a 6 on a dice). However, in the north of the area only one point was found usable due to the complex relief.

Comments about the GCPs selection:

Even if a sufficient number and a good distribution of points were finally obtained, various problems have been identified during their selection:

- The last GCPs collection dates from at least 13 years. The landscape may have changed significantly in some locations, so the points recorded in these areas are no more usable.
- The location of some points is not enough precise, centre of crossroads for example, to allow for a good repositioning.
- The points taken on elements presenting a significant elevation which are difficult to find on the acquisitions presenting a strong angle (electric pole or wall of more than 2 m).

Even if it is difficult to quantify, the elements listed above may lead to a significant pointing error of the GCPs that we estimate being around 1 meter.

5.2 Digital Elevation Model (DEM)

A DEM is used in order to correct image displacement caused by topographic relief. Therefore, used DEM should have an accuracy compatible with the resolution of VHR to be corrected.

Thus, as reported in the Guidelines for Best Practice and Quality Checking of Ortho Imagery [i], the recommendations are to use DEM:

- with maximum grid spacing of 5 to maximum 20 times the orthophoto pixel size (depending on the terrain flatness) and
- with height accuracy of 2 x planimetric 1-D RMSE

Figure 5. Relief of the study AOI

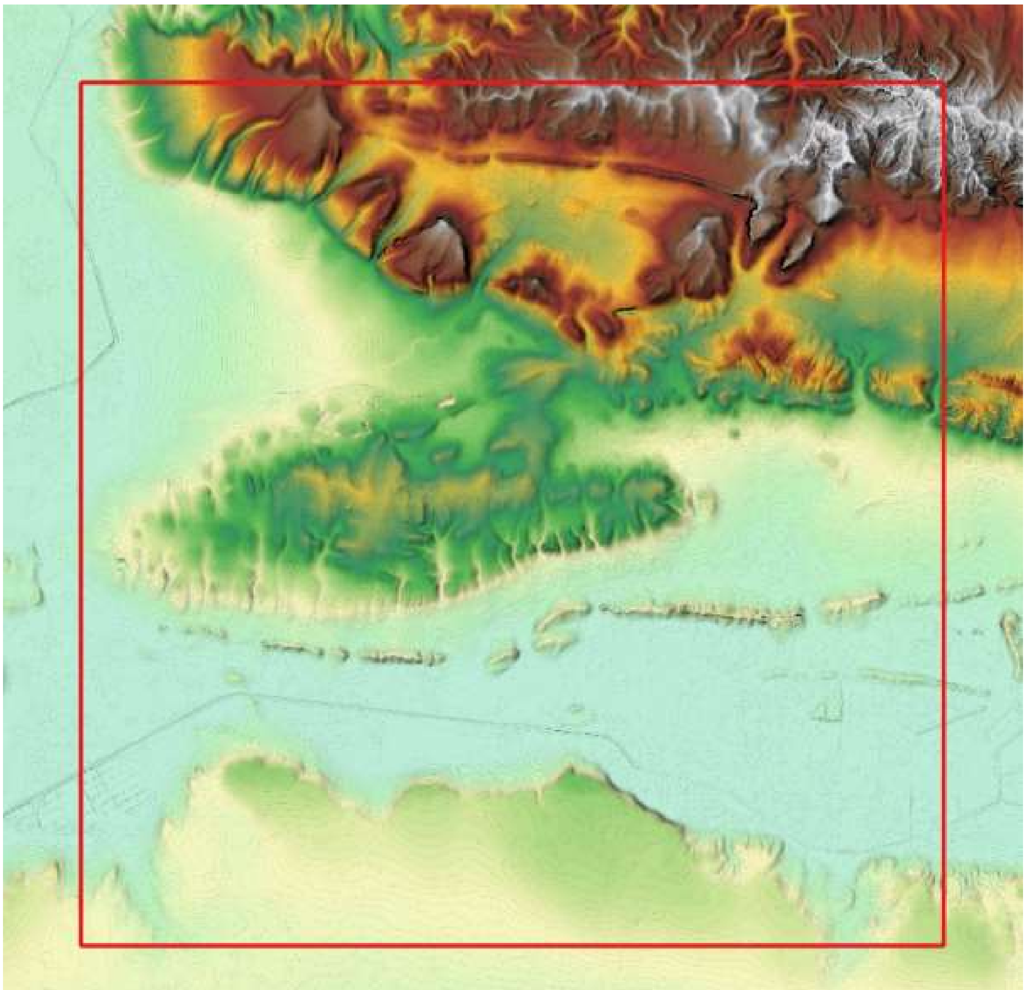

Source: JRC out of Intermap Company DEM data

The DEM used in these tests was produced by the Intermap company from Synthetic Aperture Radar (SAR) airborne shots using interferometry method.

The grid resolution of this DEM is 5M. We chose to use the DTM to avoid all the othorectification artefacts linked to the details of the DEM (tree buildings, etc.) and to the strong viewing angles which could have hindered the detection of the points in the image.

To note that a DEM should not be confused with a Digital Terrain Model (DTM) that is a topographic model of the bare earth that has vegetation, buildings, and other cultural features digitally removed, leaving just the underlying terrain.” (Intermap citation).

The DEM grid spacing and DEM height accuracy are within the requested specifications.

Table 8. ORI and CORI accuracy specifications

Pixel size	RMSE[1]	CE95[2]
1.25 m	2.0 m	4.0 m

Source: JRC

Table 9. DTM vertical accuracy specifications

DTM	Measures of Accuracy Specifications		Pixel Size / Post Spacing
Product Type	RMSE	CE95	
I	0.7 m	1.5 m	5 m
II	1.0 m	2.0 m	5 m

Source: JRC

One has to note that the data accompanying the DEM suggested that it was already at the ellipsoid. However, the first attempts at orthorectification on the ERDAS software ended in failure. After investigation by the Airbus production team, it appeared that the DTM was on the Geoid. A first step therefore consisted of referencing the altitudes on the ellipsoid thanks to the Pixel Factory system.

5.3 Aerial Orthomosaics used

Here below in ***Table 10*** are listed the details of the aerial Orthomosaics used for the work.

Table 10. Aerial Orthomosaics Specifications

Aerial Orthomosaics	Grid size	Accuracy		Projection and datum	Source
ADS40	0,5m	n/a		UTM 31N WGS84	ADS40 aerial flight by ISTAR, 2003. Bands: R, G, B, IR, PAN
Vexel UltraCam	0,5m	n/a			Vexel Ultracam aerial flight by Aerodata, 2005. Bands: R, G, B, IR, PAN

Source: JRC

5.4 Pléiades Neo satellite imagery used

To perform these benchmark test, 3 images over Maussane AOI have been acquired by each sensor with three configuration of acquisition to test the orthorectification process.

PNEO3
- NADIR acquisition with an angle of maximum 5° 19/05/2022
- MEDIUM acquisition with an angle of maximum 20° 20/02/2022
- HIGHT acquisition with an angle of maximum 30° 22/03/2022

PNEO4
- NADIR acquisition with an angle of maximum 5° 17/02/2022
- MEDIUM acquisition with an angle of maximum 20° 01/02/2022
- HIGHT acquisition with an angle of maximum 30° 11/02/2022

Table 11. Real angles of the primary product across study AOI

Sensor	Acquisition guidance	Acquisition constraints	Date	Along	Across	Viewing
PNeo3	NADIR	5	19/05/2022	-3.7	-1.3	3.9
PNeo3	MEDIUM	20	20/02/2022	-7.9	11.6	13.9
PNeo3	HIGHT	30	22/03/2022	-4.5	-25.9	26.2
PNeo4	NADIR	5	17/02/2022	-3.8	-1.3	3.9
PNeo4	MEDIUM	20	01/02/2022	3.6	-14.4	14.8
PNeo4	HIGHT	30	11/02/2022	-7.6	-25.8	26.7

Source: Airbus

Acquisitions took place from the beginning of February 2022 until May 2022. It is noted that the restricted angles requested put constraints in the acquisition attempts. Also the weather has not been favourable in spring, so the PNeo3 image at nadir could only be acquired late.
In the end, the radiometric conditions are generally good for all the acquisitions but some contain some clouds. Each acquisition was then produced with these parameters:

- Surface: limit of the AOI of 100km^2;
- Geometric processing: level sensor (primary);
- Spectral Bands combination: Pansharpened 6 bands;
- Product format: DIMAP Regular JPEG 2000;
- Pixel coding: 12 bits with basic level.

We made the choice of jpeg 2000 format to limit the size of each product (about 4.8GB).
These products have been ordered on the OneAtlas platform and produced with automatic chain of production.

Figure 6. Interface OneAtlas with order parameters

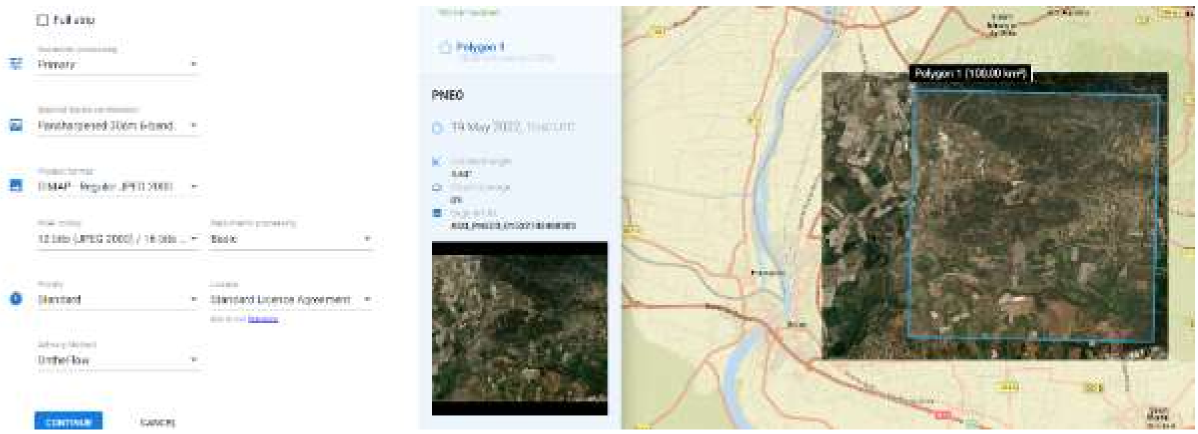

Source: Airbus

Figure 7. View in natural colour (RGB) and false colour (NED) of one acquired scene

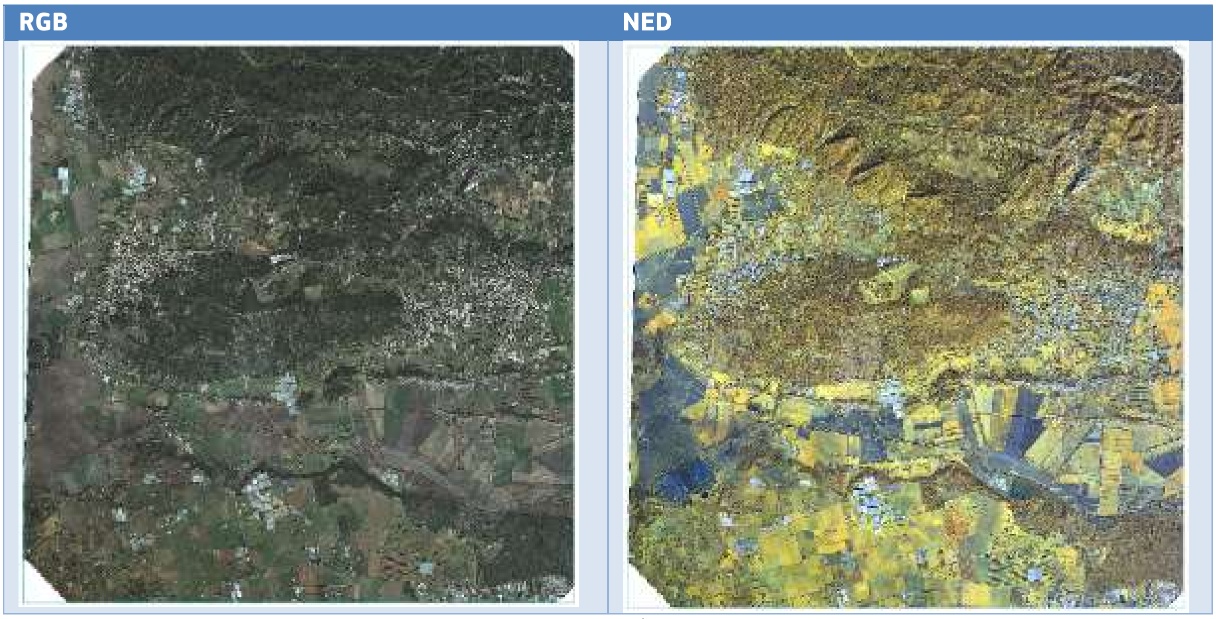

Source: Airbus

Note that the final product consists of 2 image files containing the visible RGB bands (RED, GREEN, BLUE) for the first and the NED bands (Near Infrared, Red Edge, Deep Blue) for the second. Each of these images is in turn tiled in order to limit the size of the image files.
For user-friendly use, it is preferable to set the processing software to open the images via their DIMAP file so that it can automatically manage the tiling as well as the 6 bands.

5.5 Software

To be able to carry out the orthorectifications within a short time, the choice of software was made according to the licenses available within Airbus Geo as well as the know-how present in the teams.

From the JRC work, both ENVI and Erdas imagine software were used. This choice is made since these softwares are the most commonly used in the image processing community.

- ENVI:

From the information collected under https://www.l3harrisgeospatial.com/Software-Technology/ENVI, "ENVI is an industry standard for image processing and analysis software. It is used by image analysts, GIS professionals and scientists to extract timely, reliable and accurate information from geospatial imagery. This geospatial software is scientifically proven, easy to use and tightly integrated with Esri's ArcGIS platform."

"ENVI image analysis software has remained on the cutting edge of innovation for more than three decades due in part to its support of all types of data including multispectral, hyperspectral, thermal, LiDAR and SAR. ENVI makes deep learning accessible to people through intuitive tools and workflows that don't require programming. ENVI geospatial image analysis can also be customized through an API and visual programming environment to meet specific project requirements."

We used version 5.6.1 accompanied by a patch to import the PNeo product via the DIMAP format.

- The point positioning process is quite intuitive and easy.
- It was not possible to reuse points already exported to facilitate positioning and obtain time savings in the realization of orthoimages.
- It is not possible to integrate GCPs under a cartographic projection, the points have been previously converted into geographical coordinates (wgs84).

- When processing the orthoimage, we were faced with processing stops without an error message. Parametrization tests in the calculation processing options have not been conclusive. The problem was solved by changing the hardware with newer technology RAM.
- The choices of export format are few. Only the ENVI internal format and the Geotiff are available. This forced us to carry out an additional conversion in order to export the products in JPEG2000, which is less bulky and easier to handle.
- Finally, the PNeo physical model was not ready to be integrated into the latest version of the distributed software. A solution was found thanks to the Harris Company which gave us access to its service provider in order to find a solution to produce the necessary ortho images with the rigorous model.

- Erdas Imagine:

Erdas Imagine is an image processing software and a GIS distributed by Hexagon company (https://hexagon.com/products/erdas-imagine)

"ERDAS IMAGINE provides true value, consolidating remote sensing, photogrammetry, LiDAR analysis, basic vector analysis, and radar processing into a single product."

We used version 2022 of Erdas Imagine accompanied by a patch to import the PNEO product via the DIMAP format.

The older interface of ERDAS was more complicated to understand but ultimately offers more ease of adaptation to its working environment.

6 Pléiades Neo Benchmarking Tests

6.1 Benchmarking Methodology

Orthorectification of images is a process to apply corrections for optical distortions from the sensor system, and apparent changes in the position of ground objects caused by the perspective of the sensor view angle and ground terrain. This process usually consists of 3 phases:

Phase 1: Modelling - geometric correction model phase, also referred as to image correction phase, sensor orientation phase, space resection or bundle adjustment phase. Sensor models are mathematical models that define the physical relationship between image coordinates and ground coordinates, and they are different for each sensor. In this phase Ground Control Points are used for improving absolute accuracy. However, the tests were also performed without using GCPs.

Phase 2: Orthorectification - the phase where distortions in image geometry caused by the combined effect of terrain elevation variations and non-vertical angles from the satellite to each point in the image at the time of acquisition are corrected.

Phase 3: External Quality Control (EQC) of the final product - described by 1-D RMSEx and 1-D RMSEy – performed by JRC. According to Guidelines for Best Practice and Quality Checking of Ortho Imagery [i] minimum 20 check points should be checked to assess ortho image planimetric accuracy. The points used during the geometric correction phase should be excluded.

Figure 8. Standard benchmarking procedure

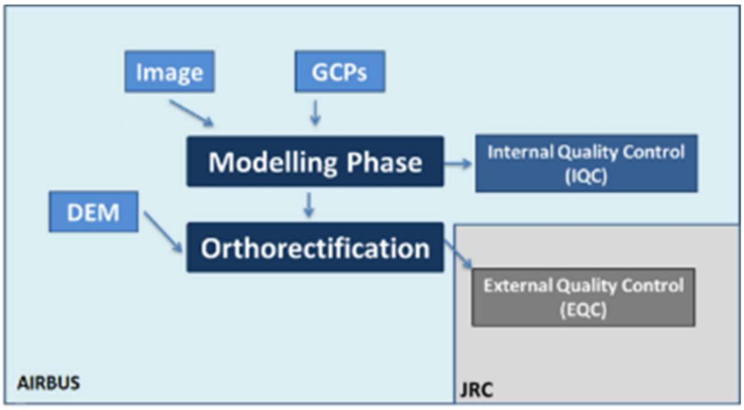

Source: JRC

6.2 Test Scenarios

The following scenarios have been considered in our benchmarking tests:

Table 12. Tested Scenarios

IMAGES	DEM	GCP #	model	ERDAS	ENVI	PNeo3	PNeo4	TOTAL
PNeo3/4 close nadir	Intermap	0	RPC (0)	1	1	1	1	4
		3		1	1	1	1	4
		4		1	1	1	1	4
PNeo3/4 close nadir	Intermap	6	Rigorous	1	1	1	1	4

PNeo3/4 medium	Intermap	0	RPC (0)	1	1	1	1	4
		3		1	1	1	1	4
		4		1	1	1	1	4
PNeo3/4 medium	Intermap	6	Rigorous	1	1	1	1	4
PNEO3/04 high	Intermap	0	RPC(0)	1	1	1	1	4
		3		1	1	1	1	4
		4		1	1	1	1	4
		6		1	1	1	1	4
PNEO3/04 high	Intermap	6	Rigorous	1	1	1	1	4
		9		1	1	1	1	4
Total								**56**
IMAGES	**DEM**	**angle**	**model**		**ENVI**	**PNeo3**	**PNeo4**	**TOTAL**
PNeo3/4	Airbus DEM	low	automatic ortho by Airbus (no GCPs)		1	1	1	2
		medium			1	1	1	2
		high			1	1	1	2
Total								**6**

Source: JRC

62 test products were carried out with the 6 images equally between the PNeo3 and PNeo4 sensors.

The organization of work is carried out in 7 batches even if foreseen order could not be respected depending on the availability of acquisitions or software.

The same tests were carried out for each sensor.

Acquisitions with a high angle were tested more than acquisitions at nadir and medium acquisition angle. It represents 42% of the tests against 29% for each of the other 2 types of medium and nadir angles.

The number of tests done with ENVI and ERDAS is the same. Note that the 6 tests done on the airbus chain, whose production is in automatic mode, could not allow following the same test processes as for ENVI and ERDAS software.

Regarding the GCPs, 5 test configurations were performed with 0, 3, 4, 6 and 9 GCPs. The configuration with 6 GCPS was the most tested 26% and that with 9 GCPs the least tested 6%. The configurations with 0, 3 and 4 GCPs have the same number of tests and each represents 19% of the tests. Note the presence of 6 Airbus products which have been produced in automatic mode.

Finally, 2 modelling modes were used. The first, RPC, represents 65% of the tests and the second, rigorous modelling, represents 16% of the tests.

Table 13. Distribution of tests according to parameters

		test number	total by parameter
sensor	PNeo3	31	62
	PNeo4	31	
acquisition angle	low	18	62
	medium	18	
	hight	26	
software	Airbus chain	6	62
	ENVI	28	
	ERDAS	28	
GCP number	0	12	62
	3	12	
	4	12	
	6	16	
	9	4	
	Auto (airbus)	6	
model	RPC	40	62
	rigourous	16	
	AirbusDS	6	

Source: JRC

6.3 Internal Quality Control (Airbus)

The modelling results provided by each software were checked during each orthorectification process.

However, the difficulty of exporting these results during orthorectification did not make it possible to have an overview and a comparison of these results.

Airbus has implemented an internal control to check the quality of:

- statement of the coordinates of 10 independent GCPs on all the orthorectifications;
- measurement of difference in x and y with respect to the initial coordinates of each GCP;
- calculation of the RMSEx and the RMSEy.

Table 14. Acquired Images

image	rmse_x	rmse_y	angle	model	sensor	soft
B0_P4_hight_AIRBUS_20220211	1,28	1,43	hight		P4	Airbus
B1_P3_hight_ENV_0_RCP_20220322	1,29	0,81	hight	RCP	P3	ENV
B1_P4_hight_ENV_0_RCP_20220211	1,45	1,61	hight	RCP	P4	ENV
B1_P4_hight_ERD_0_RCP_20220211	1,29	1,45	hight	RCP	P4	ERD
B0_P3_medium_AIRBUS_20220220	2,38	1,03	medium		P3	Airbus
B5_P3_medium_ENV_0_RCP_20220220	1,96	1,16	medium	RCP	P3	ENV
B5_P3_medium_ERD_0_RCP_20220220	1,95	1,11	medium	RCP	P3	ERD

Source: Airbus

Only 3 images (out of 62) exceed the threshold of 1.25 for the RMSEx and the RMSEy and another 4 other images only exceeding the threshold of 1.25 RMSEx.

Of these 7 images, 2 are part of the 6 orthorectification products carried out on the automatic and standard Airbus processing chain.

As mentioned previously, we consider that the pointing error of some GCPs can reach 1 meter. This pointing error can affect both on the GCPs used for the orthorectification product of the images as well as on those used for internal and external control. This aspect must therefore be taken into account when reading these results. Also, the Airbus processing chain was still under development and not finalised at the time of the benchmarking study.

Impact of sensors

Figure 9. RMSEx and RMSEy depending on the sensor

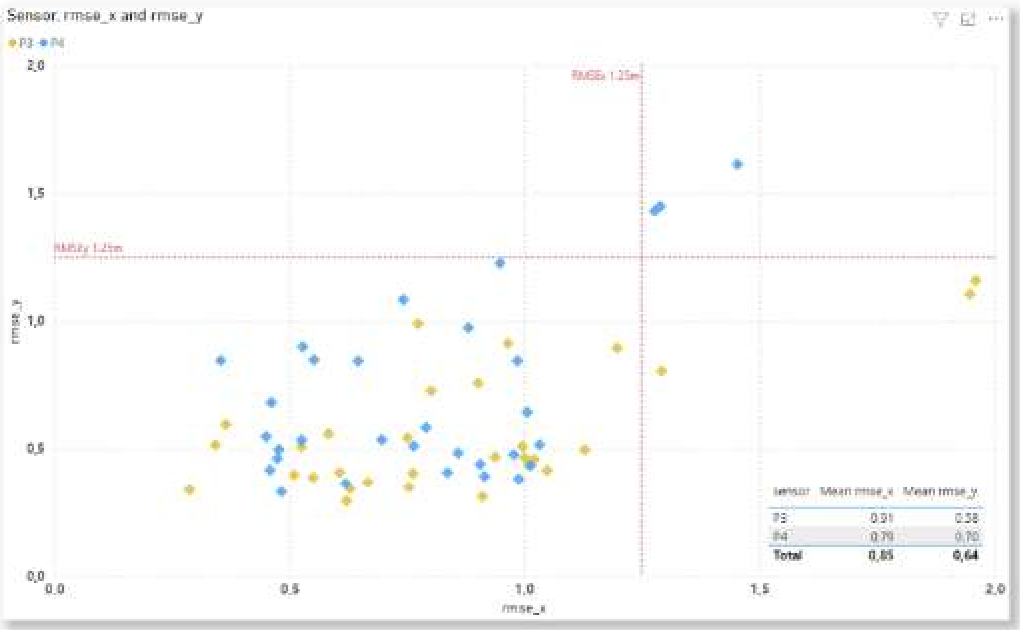

Source: Airbus

On ***Figure 9*** we can note similar results for the 2 sensors if even the results are slightly better for PNeo3 in y 0,58m versus 0,7m7 for PNeo4.

Impact of acquisition angle

Figure 10. RMSEx and RMSEy depending on the acquisition angle

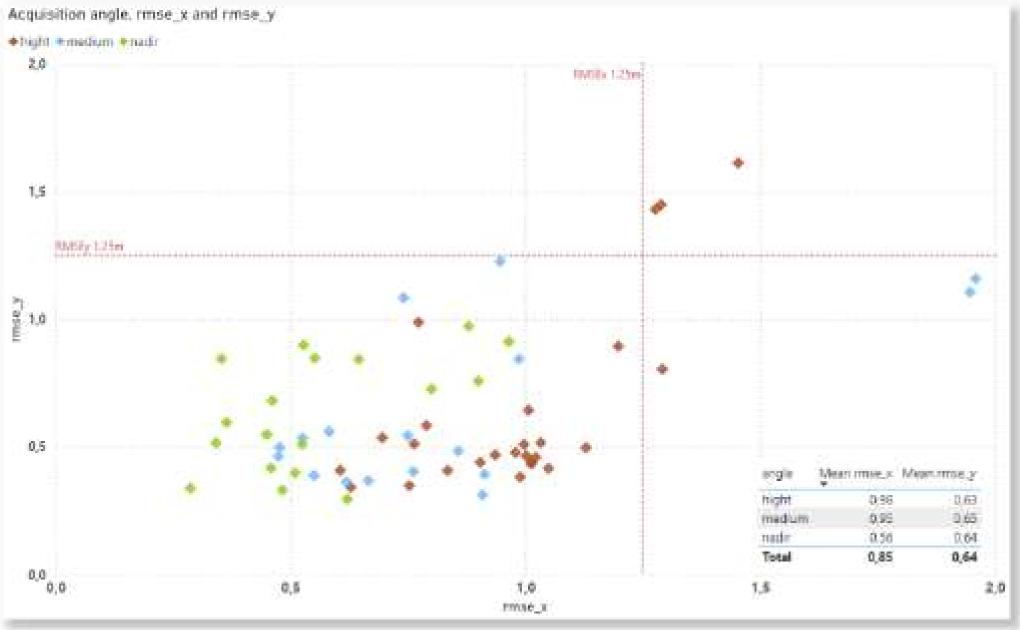

Source: Airbus

As expected the test shows that the distribution of RMEx and RMSEy errors is increasing while getting off nadir acquisitions. Some points are out of threshold accuracy in the medium and high acquisition angles. This phenomenon should be monitored in the future.

Impact of models (RPC or rigorous)

Figure 11. RMSEx and RMSEy depending on the orthorectification model used

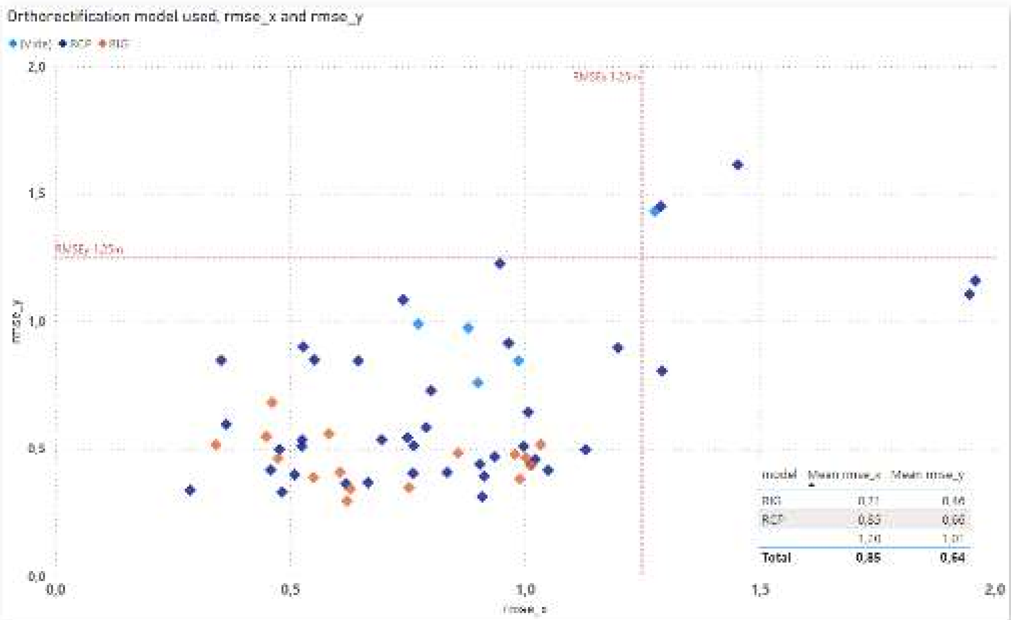

Source: Airbus

The images orthorectified via the rigorous model are of better quality. The difference between rigorous model and RPC is very noticeable in the direction of axis y. However, the reason for this difference was not further investigated since it was not part of the scope of the benchmark work.

Impact of GCPs number

Figure 12. RMSEx and RMSEy depending on the number of GCPs used

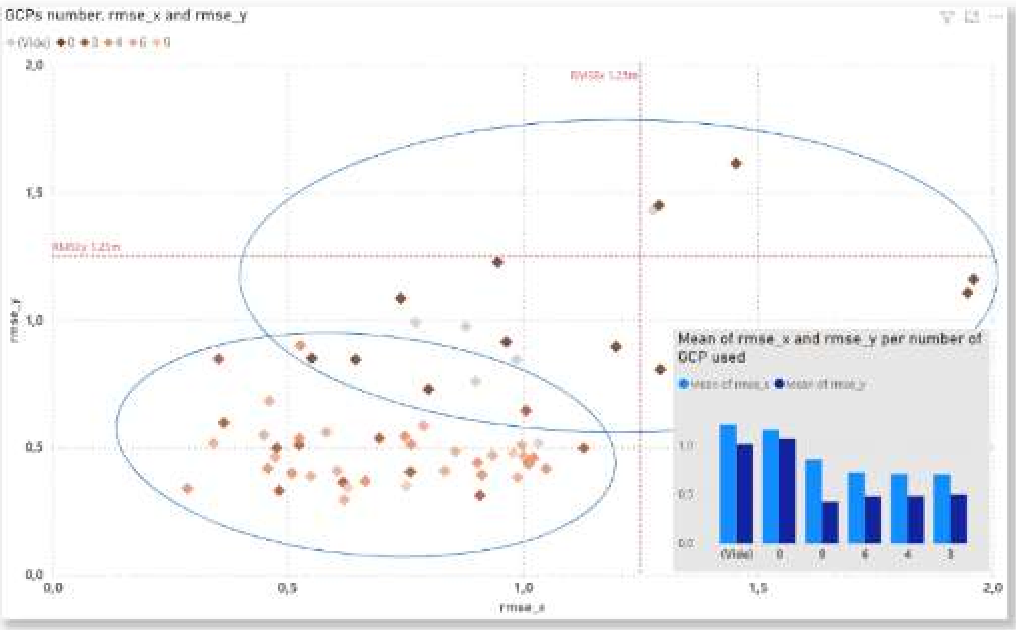

Source: Airbus

Without GCPs the RMSEx and RMSEy are close to 1.1m.

As expected, the use of GCPs allows improving the positional accuracy. However, with the set of GCPs available, when further increasing their number, we observed an improvement of the localization in y, but a deterioration of the localization in x. Since it is not part of the main scope of the benchmarking tests, this has not been further investigated to possibly identify the reason(s) of this behaviour.

Impact of Software

Figure 13. RMSEx and RMSEy depending on the number of GCPs used

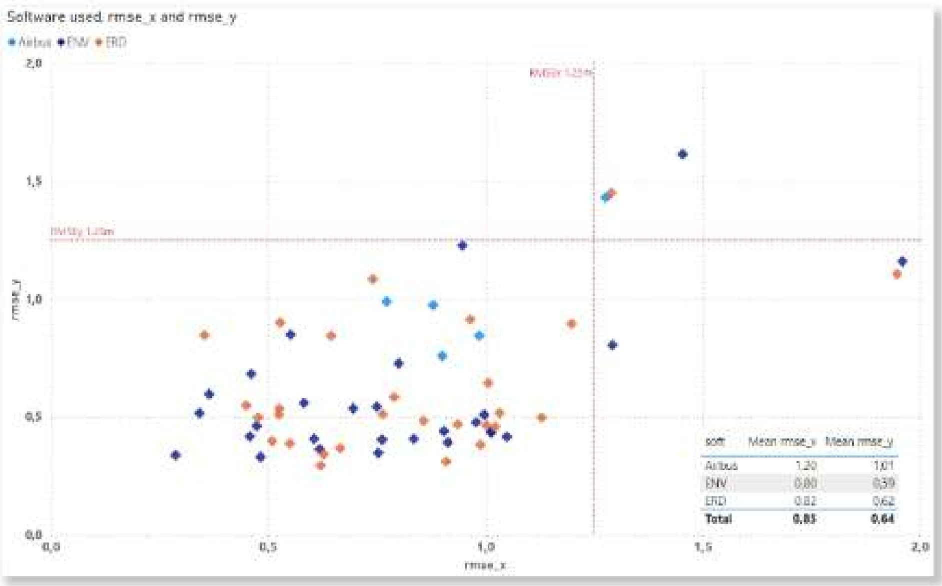

Source: Airbus

The difference between the ortho products of ERDAS Imagine and ENVI are minimal. Airbus software provides less accurate results since their automatic processing chain in place does not use GCPs.

To check the proper performance of the 3 softwares, a comparison should be done with results obtained with no GCPs used. Due to lack of time this comparison has not been done.

7 External Quality Control

JRC as an independent entity performs a validation phase of the benchmarking workflow methodology used for verifying of a satellite's ortho-product compliance with the geometric quality criteria set up for the Control with Remote Sensing program (CwRS), in Common Agriculture Policy (CAP). The workflow follows the Guidelines for Best Practice and Quality Checking of Ortho Imagery [i] and is in detail described in the chapter 6.1.

7.1 Method for external quality check (EQC) of ortho imagery

7.1.1 Independent check points (ICPs) selection and distribution

For the evaluation of the geometric accuracy of the PNeo ortho imagery, 22 ICPs were selected by a JRC operator. Both GCPs and ICPs were retrieved from already existing datasets of differential global positioning system (DGPS) measurements over Maussane test site. These datasets were updated and maintained by JRC until 2012. Considering the accuracy, distribution and recognisability on the given images, points from the three datasets were used for the EQC. The intention is to obtain points evenly distributed across the whole image while keeping at least the minimum recommended number of 20 points [i]. For the location of the ICPs, JRC took into account the distribution of the GCPs used by Airbus and provided to JRC together with the products. Since the measurements on ICPs have to be completely independent (i.e. ICP must not correspond to GCP used for correction) GCPs taken into account in the geometric correction have been excluded from the datasets considered for EQC.

Regarding the positional accuracy of ICPs, according to the Guidelines [i] the ICPs should be at least 3 times (5 times recommended) more precise than the target specification for the ortho, i.e. in our case of a target 1.25m RMS error (the most strict value was taken into account here) the ICPs should have a specification of 0.42m (0.25m recommended). 21 ICPs that have been selected fulfil the defined criteria and 1 ICP is slightly above the mentioned threshold (***Table 15***, ***Table 16***).

Table 15. Identical check points specifications

Dataset	RMSEx [m]	RMSEy [m]	N.of points
ADS40_GCP_dataset_Maussane 2003	0,05	0,10	1
VEXEL_GCP_dataset_Maussane 2005	0,49	0,50	1
Multi-use_GCP_dataset_Maussane 2009	0,30	0,30	15
Maussane GNSS field campaign 2012	< 0,15	< 0,15	5

Source: JRC

Figure 14. ICPs dataset used by JRC in the EQC of PNeo ortho imagery.

Source: JRC with Airbus PNeo background image

Table 16. ICPs overview

ID	E[m]	N[m]
C4R5NEW	64507924.00	484001539.00
C4R4	64531764.00	484323364.00
110013	639418.26	4840602.35
66063	636896.93	4842180.72
66046	641148.67	4837348.79
C2R4	63782972.00	484360987.00
C3R5NEW	64034136.00	483888755.00
C3R4	64160872.00	484312915.00
66010	643598.10	4845690.29
66004	636363.62	4846077.52
66020	637261.09	4837987.96
66022	637947.95	4837300.70
66014	645687.64	4845487.95

66011	644844.93	4844945.47
66016	636347.01	4837279.93
440003	640999.13	4845715.57
66031	644655.96	4839947.67
66025	641380.52	4841215.07
66024	641320.70	4838276.56
66026	640049.05	4840996.07
66035	644717.26	4837489.03

Source: JRC

The projection and datum details of the above mentioned data are UTM 31N zone, WGS 84 ellipsoid.

7.1.2 Geometric quality assessment-measurements and calculations

Geometric characteristics of orthorectified images are described by Root-Mean-Square Error (RMSE) RMSEx (easting direction), RMSEy (northing direction) and CE(90), calculated for a set of Independent Check Points.

$$RMSE_x = \mathrm{RMSE}_{1\mathrm{D}}(East) = \sqrt{\frac{1}{n}\sum_{i=1}^{n}\left(X_{REG(i)} - X_{(i)}\right)^2}$$

$$RMSE_y = \mathrm{RMSE}_{1\mathrm{D}}(North) = \sqrt{\frac{1}{n}\sum_{i=1}^{n}\left(Y_{REG(i)} - Y_{(i)}\right)^2}$$

where X,YREG(i) are ortho imagery derived coordinates, X,Y(i) are the ground true coordinates, n express the overall number of ICPs used for the validation.

This geometric accuracy representation is called the positional accuracy, also referred to as planimetric/horizontal accuracy and it is based on measuring the residuals between coordinates detected on the ortho image and the ones measured in the field or on a map of an appropriate accuracy.

According to ISO 19157, the circular error at 90% CE(90) significant level (or confidence interval) is defined as a radius describing a circle, in which the true point location lies with the probability of 90 %. It is also known as CMAS (circular map accuracy standard).

$$\mathrm{CE}(90) = 2{,}146\,\frac{\sqrt{RMSE(East)^2 + RMSE(North)^2}}{\sqrt{2}}$$

If the error is normally distributed in each the x- and y-component, the error for the x-component is equal to and independent of error for the y-component, and sufficient check points are available to accurately estimate the variances, CE90 can be expressed as 2,146 times the one dimensional root mean square error:

$\mathrm{CE}(90) = 2{,}146 * RMSE_{(East)}$ or $\mathrm{CE}(90) = 2{,}146 * RMSE_{(North)}$

Unlike the values obtained from the field measurements (in our case with GPS device) which are of the defined accuracy the coordinates registered from the involved ortho images are biased by various influencing factors (errors of the source image, quality of auxiliary reference data, visual quality of the image, experience of an operator etc..). It should be taken into account that all these factors are then subsequently reflected in the overall RMSE which in practice aggregates the residuals into a single measure.

All measurements presented were carried out in ERDAS Imagine 2016 software, using Metric Accuracy Assessment. Protocols from the measurements contain other additional indexes like mean errors or error standard deviation that can also eventually help to better describe the spatial variation of errors or to identify potential systematic discrepancies [i].

Since the JRC datasets of DGPS points are of a high variety as for the date of origin is concerned (2003-2012) many points were difficult to detect due to the meanwhile change of the overall landscape. Also, the ADS40 aerial orthomosaic is 19 years old and therefore does not always correspond to the actual state of the region. Thus, for the selection of some ICPs on the ortho images the other complementary sources to the aerial image were used, like for instance previously orthorectified VHR images or Google Earth 2D sequences, which helps to follow the change of the situation during the years, for some cases (where available) also 3D view.

Due to the fact that JRC datasets are obsolete (i.e. some GCPs/ICPs are difficult to identify, an example is point 66007 which is not included in the analysis due to very high discrepancies) the results may be encumbered with additional errors.

8 Results and discussions

Results of the quality control are presented hereafter under different forms and formats in order to illustrate and discuss the possible impact of factors intervening in the final positional accuracy such as the sensors, the GCPs, the acquisition angle, the image processing software or even the ortho correction model.

8.1 Impact of the orthorectification model

In ***Table 17*** and ***Table 18*** are provided the results of the QC using the Rational Function modelling for the PNeo3 and PNeo4 sensors respectively.

Table 17. Obtained quality control results (RMSE1D) on ortho image produced by applying Rational Function Modelling, using JRC ICPs dataset – PNeo3

ONA (Off Nadir Angle)	**RPC model**	**ERDAS**		**ENVI**	
	GCPs	**RMSEx ERDAS**	**RMSEy ERDAS**	**RMSEx ENVI**	**RMSEy ENVI**
5°	0	0.81	1.02	0.79	0.95
	3	0.89	0.82	0.88	1.05
	4	0.75	0.78	0.82	0.89
20°	0	1.99	1.40	1.92	1.48
	3	0.78	0.84	0.94	0.67
	4	0.72	0.72	0.99	0.59
30°	0	1.03	0.99	1.12	0.87
	3	1.27	0.74	1.30	0.60
	4	1.06	0.73	1.34	0.68
	6	1.01	0.63	1.68	0.65

Source: JRC

Table 18. Obtained quality control results (RMSE1D) on ortho image produced by applying Rational Function Modelling, using JRC ICPs dataset – PNeo4

ONA	RPC model	ERDAS		ENVI	
	GCPs	**RMSEx ERDAS**	**RMSEy ERDAS**	**RMSEx ENVI**	**RMSEy ENVI**
5°	0	0.70	0.78	0.56	0.80
	3	0.58	0.70	0.87	0.76
	4	0.66	0.77	0.98	0.55

20˚	0	1.32	1.11	1.52	1.28
	3	1.13	0.90	0.98	0.72
	4	1.03	0.87	1.08	0.84
30˚	0	1.69	1.26	1.87	1.96
	3	1.23	0.98	1.16	0.92
	4	1.01	0.73	1.45	0.80
	6	0.97	0.74	1.39	0.82

Source: JRC

In ***Table 19*** and ***Table 20*** are provided the results of the QC using the Rigorous model for the PNeo3 and PNeo4 sensors respectively.

Table 19. Obtained quality control results (RMSE1D) on ortho image produced by applying Rigorous Modelling, using JRC ICPs dataset – PNeo3

	Rigorous model	ERDAS		ENVI	
ONA	GCPs	RMSEx ERDAS	RMSEy ERDAS	RMSEx ENVI	RMSEy ENVI
5	6	0.76	0.69	0.71	0.74
20	6	0.86	0.74	0.77	0.76
30	6	0.90	0.67	0.68	0.64
	9	1.01	0.69	1.13	0.66

Source: JRC

Table 20. Obtained quality control results (RMSE1D) on ortho image produced by applying Rigorous Modelling, using JRC ICPs dataset – PNeo4

	Rigorous model	ERDAS		ENVI	
ONA	GCPs	RMSEx ERDAS	RMSEy ERDAS	RMSEx ENVI	RMSEy ENVI
5	6	0.81	0.71	0.89	0.73
20	6	1.21	0.77	0.99	0.79
30	6	1.27	0.85	1.32	0.75
	9	1.25	0.83	1.38	0.70

Source: JRC

In ***Figure 15*** and ***Figure 16*** are reported the planimetric RMSE 1D errors for the PNeo3 and PNeo4 sensors respectively.

Figure 15. Point representation of planimetric RMSE 1D errors calculated on ortho images using JRC ICPs dataset for PNeo3

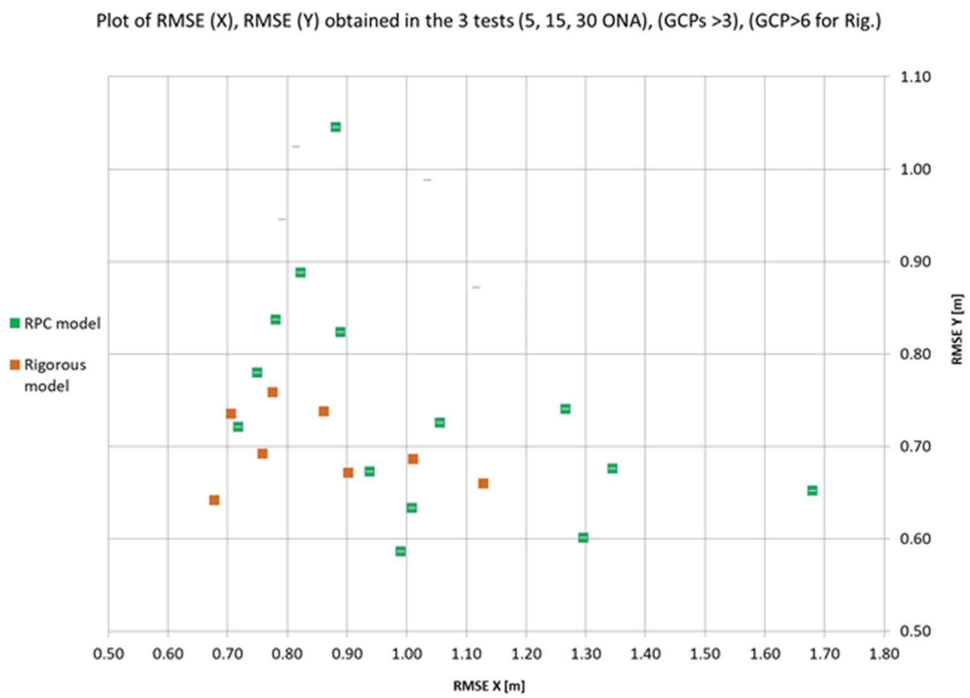

Source: JRC

Figure 16. Point representation of planimetric RMSE 1D errors calculated on ortho images using JRC ICPs dataset – PNeo4

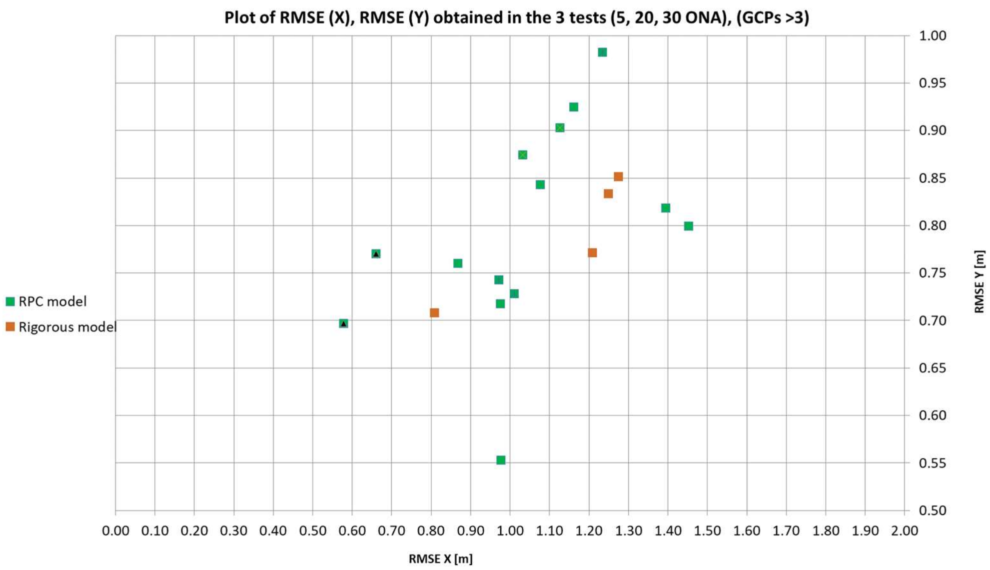

Source: JRC

From the ***Table 17*** to ***Table 20*** we can summarize that RMSE values obtained with RPC based ortho images and rigorous ones are very similar, for equivalent number of GCPs used. We can conclude that both models can be equally used without impacting on results. Nevertheless, from ***Figure 15*** and ***Figure 16***, one can see that with the rigorous model, results are a bit less scattered than with RPC.

8.2 Impact on the number of GCPs used for the image processing

In ***Figure 17*** to ***Figure 22*** below are presented the RMSEs measured using the RPC model for different number of GCPs using ERDAS and ENVI software for 3 types of acquisition angle (5, 20 and 30 degrees off-nadir angles) and for sensors PNeo3 and PNeo4.

In ***Figure 23*** and ***Figure 24*** are presented the results using the rigorous model for the 30 degrees off-nadir angle and both sensors PNeo3 and PNeo4.

Figure 17. Behaviour of RMSEs across the various number of GCPs for ERDAS and ENVI software, source image 5˚off nadir – PNeo3, RPC modelling

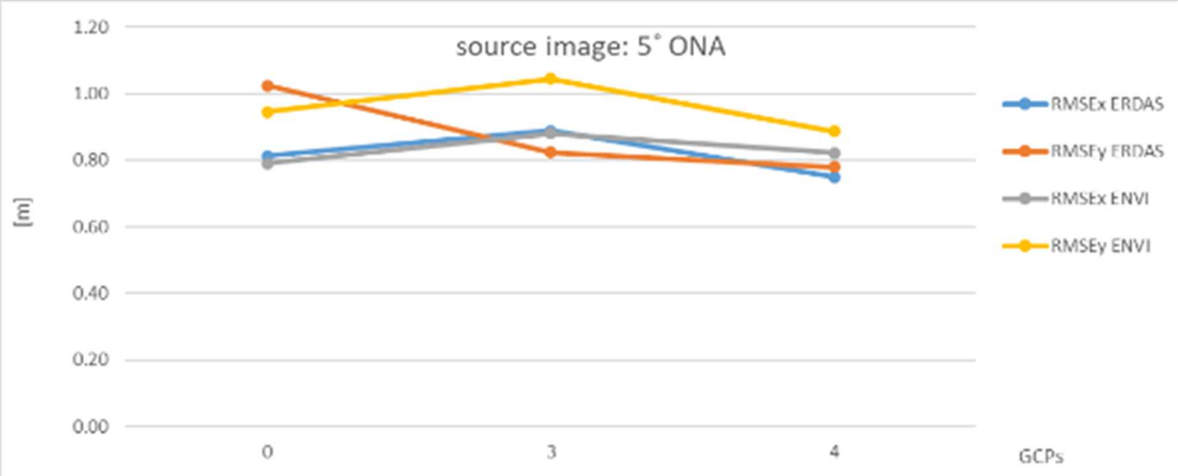

Source: JRC

Figure 18. Behaviour of RMSEs across the various number of GCPs for ERDAS and ENVI software, source image 5˚off nadir – PNeo4, RPC modelling

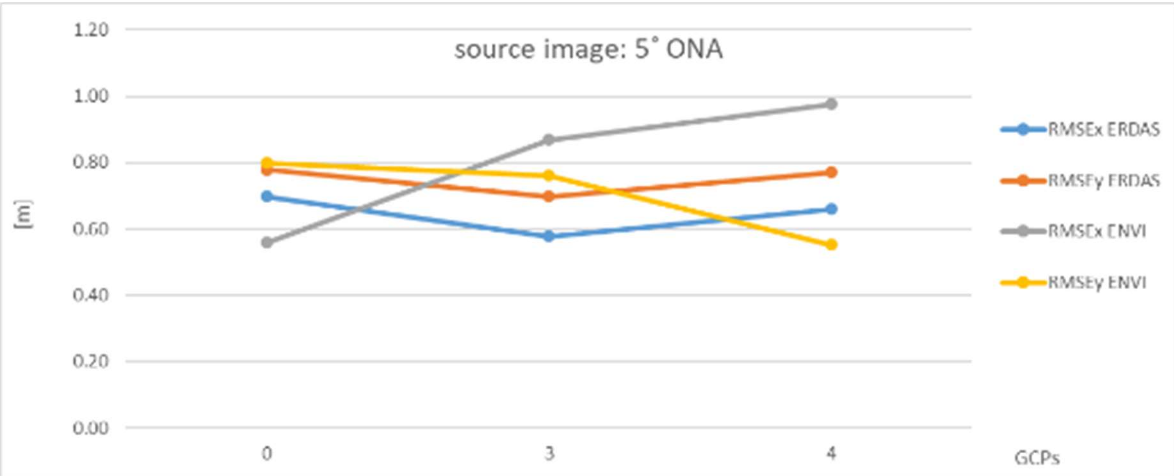

Source: JRC

Figure 19. Behaviour of RMSEs across the various number of GCPs for ERDAS and ENVI software, source image 20˚off nadir – PNeo3, RPC modelling

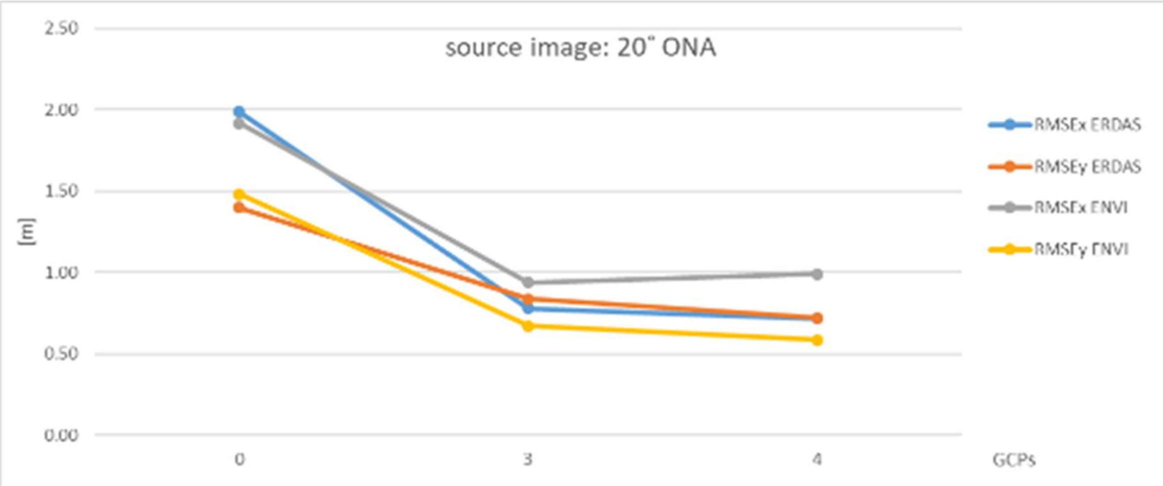

Source: JRC

Figure 20. Behaviour of RMSEs across the various number of GCPs for ERDAS and ENVI software, source image 20˚off nadir – PNeo4, RPC modelling

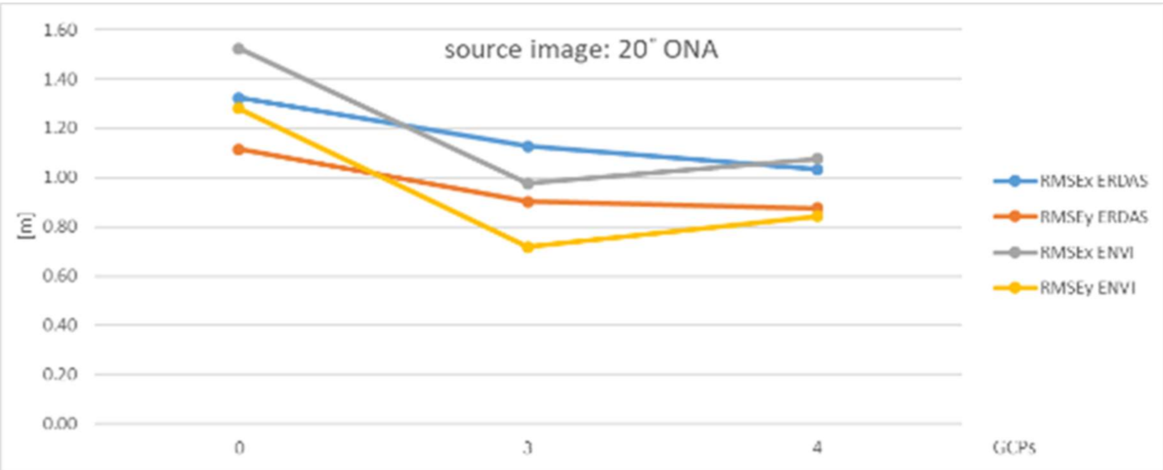

Source: JRC

Figure 21. Behaviour of RMSEs across the various number of GCPs for ERDAS and ENVI software, source image 30˚off nadir – PNeo3, RPC modelling

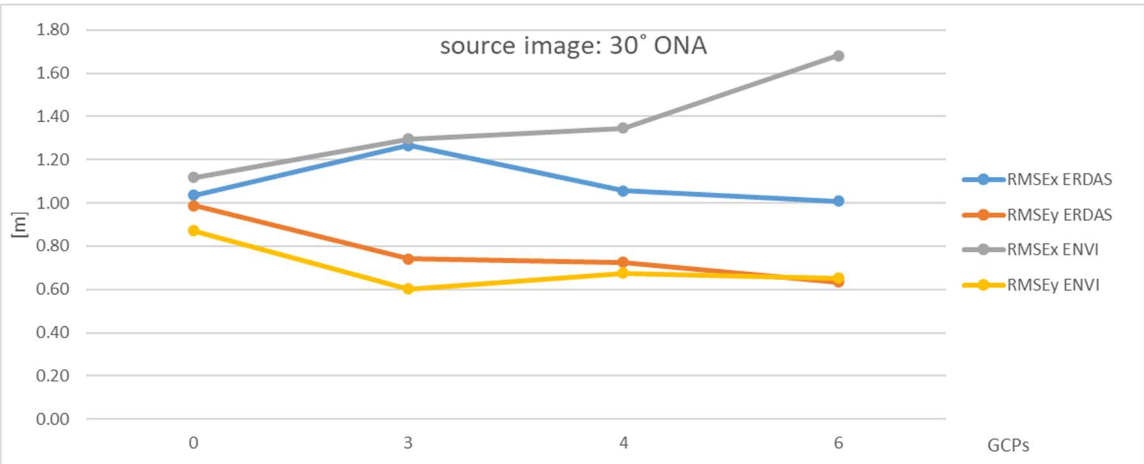

Source: JRC

Figure 22. Behaviour of RMSEs across the various number of GCPs for ERDAS and ENVI software, source image 30˚off nadir – PNeo4, RPC modelling

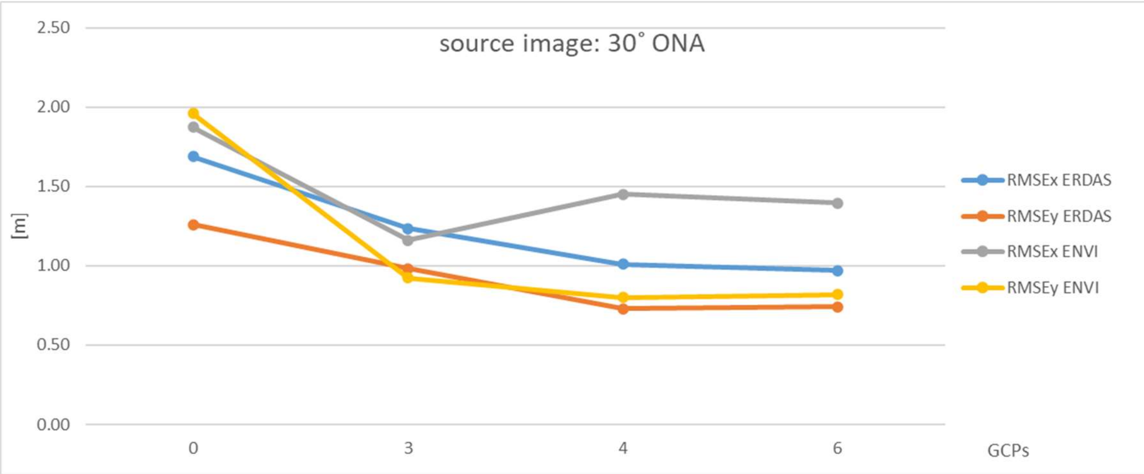

Source: JRC

Figure 23. Behaviour of RMSEs across the various number of GCPs for ERDAS and ENVI software, source image 30˚off nadir – PNeo3, Rigorous modelling

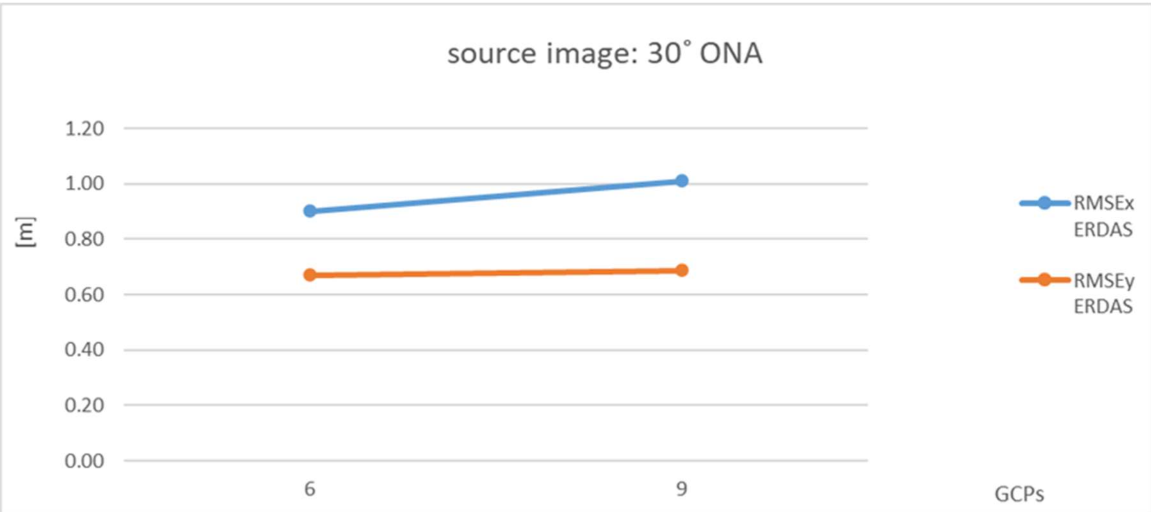

Source: JRC

Figure 24. Behaviour of RMSEs across the various number of GCPs for ERDAS and ENVI software, source image 30˚off nadir – PNeo4, Rigorous modelling

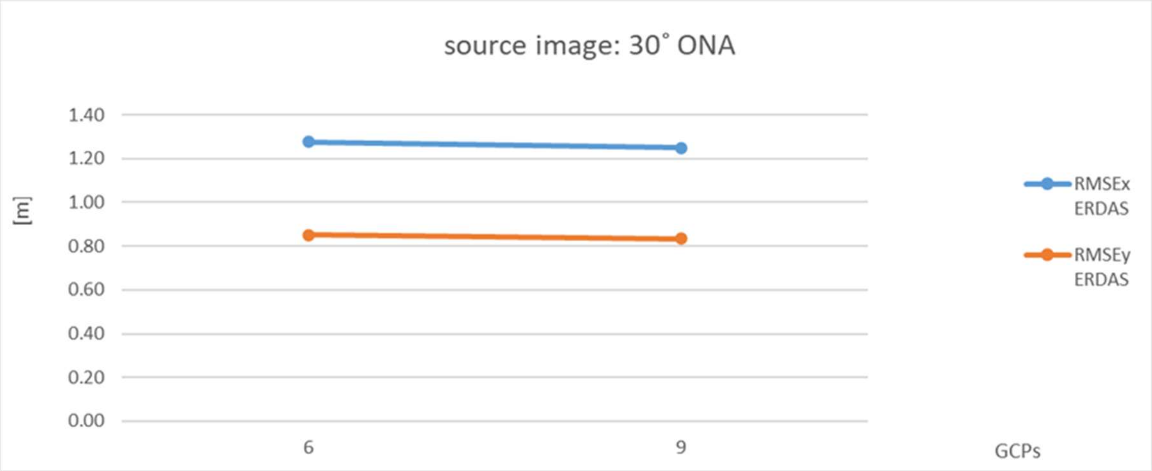

Source: JRC

Looking at the above ***Figure 17*** to ***Figure 24*** we can draw the following conclusions and recommendations:

- As expected the number of GCPs is impacting the quality and accuracy of the orthorectification process;
- With Pléiades Neo images, apart for acquisition <5º off-nadir, it is recommended to always use a minimum of 3 GCPs when using RPC modelling to possibly obtain an orthophoto within requested accuracy;
- Nevertheless, still using RPC modelling, a further increase of number of GCPs (i.e. higher than 3 GCPs) does not bring substantial improvement of RMSE values;
- When applying the rigorous model, there is a need to use at least 6 GCPs, but then also for this model, a further increase of GCP number does not improve significantly the positioning accuracy.

In the ***Table 21*** below, are reported the results obtained with the orthoimagery produced by the Airbus automatic chain. At the time of the work, the automatic processing chain was still under development and was operating without using any GCPs. One can observe that results are often out of specification when acquisition angle is > 5º off-nadir.

Table 21. Obtained quality control results (RMSE1D) on ortho images produced by applying Airbus automatic chain, using JRC ICPs dataset – PNEO 3 and PNEO 4

	PNeo 3		PNeo 4	
ONA	RMSEx	RMSEy	RMSEx	RMSEy
5	0.71	0.81	0.68	0.89
20	2.32	1.24	1.41	1.09
30	1.14	1.00	1.61	1.74

Source: JRC

8.3 Impact of software used

Looking at ***Figure 17*** to ***Figure 22*** we can summarize that both software (ERDAS, ENVI) produce ortho imagery of a very similar geometric accuracy. To note that for ENVI software the RMSEx, when acquisition angle is 30º off-nadir, seems to provide anomalous values. This should be further investigated, but there was not a sufficient number of images available, nor the time available to do.

8.4 Impact of image acquisition angles

In **Figure 25** *to*

Figure 28 below are presented, in a different way that figures 17 to 22, the RMSEs obtained with RPC and rigorous models with Erdas and ENVI software, for 3 types of acquisition angle (5, 20 and 30 degrees off-nadir angles) and using different number of GCPs and thus for the sensor Pléiades Neo 3.

Figure 29 to ***Figure 32*** provide the same elements by for Pléiades Neo 4 sensor.

Figure 25. Graph of RMSEs as a function of the number of GCPs and off nadir angle, ERDAS software, RPC modelling, Pléiades Neo 3

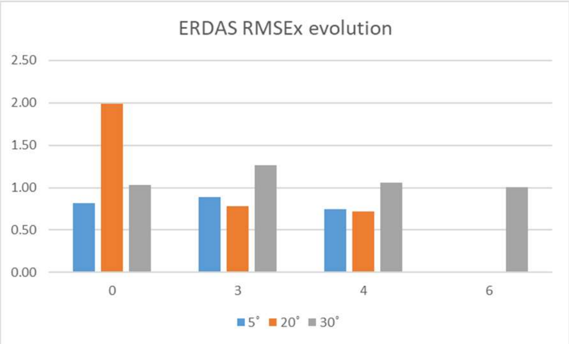

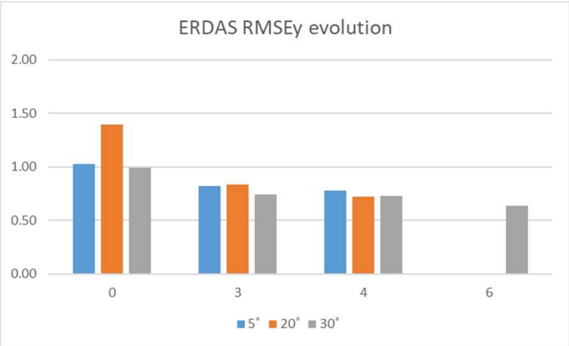

Source: JRC

Figure 26. Graph of RMSEs as a function of the number of GCPs and off nadir angle, ENVI software, RPC modelling, Pléiades Neo 3

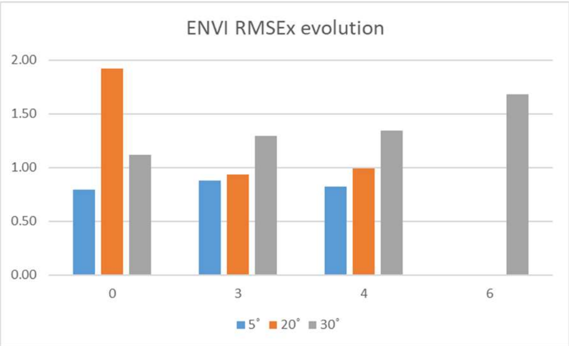

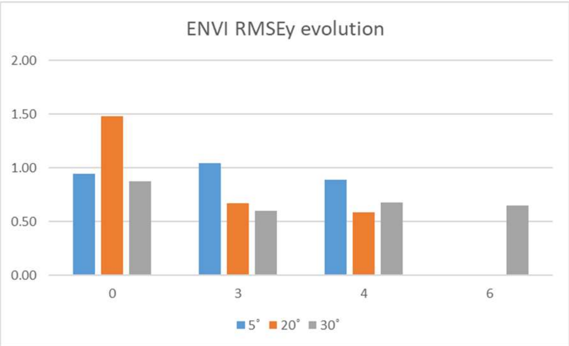

Source: JRC

Figure 27. Graph of RMSEs as a function of the number of GCPs and off nadir angle, ERDAS software, Rigorous modelling, Pléiades Neo 3

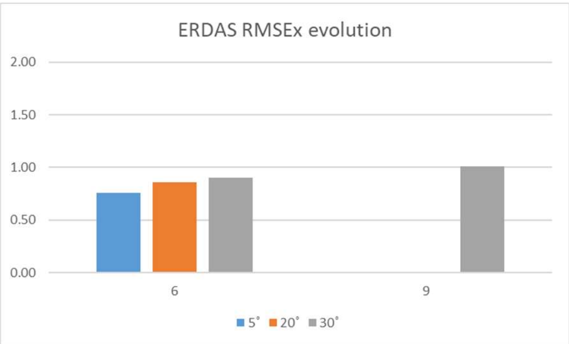

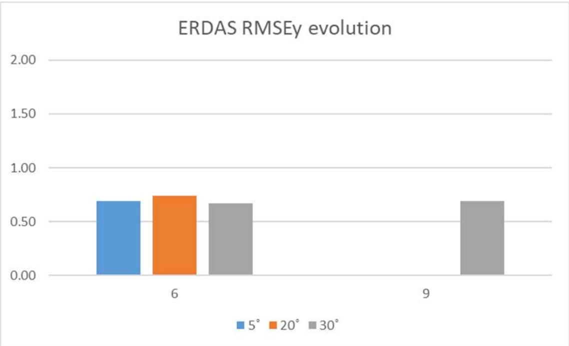

Source: JRC

Figure 28. Graph of RMSEs as a function of the number of GCPs and off nadir angle, ENVI software, Rigorous modelling, Pléiades Neo 3

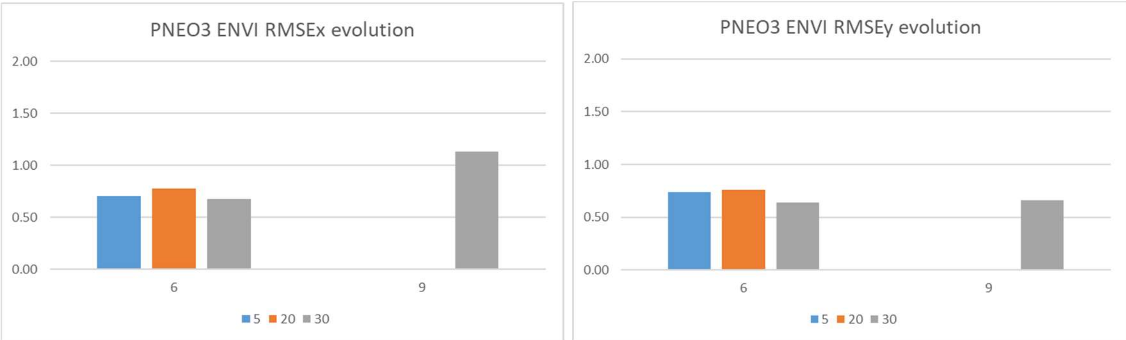

Source: JRC

Figure 29. Graph of RMSEs as a function of the number of GCPs and off nadir angle, ERDAS software, RPC modelling, Pléiades Neo 4

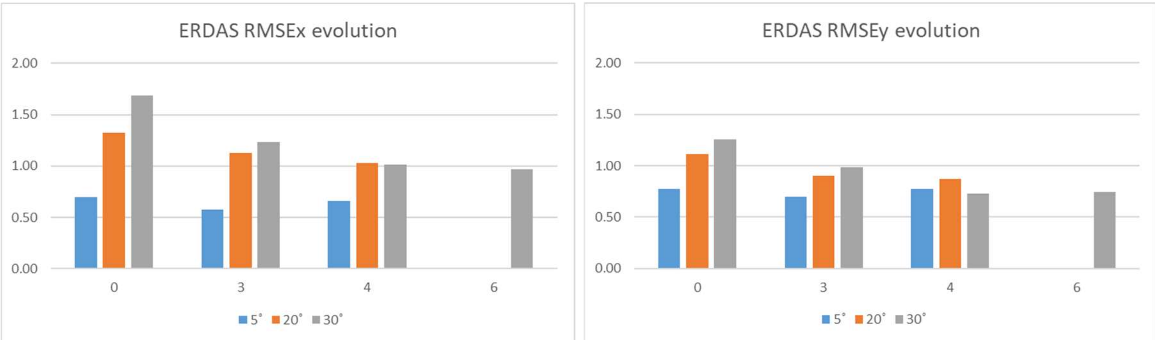

Source: JRC

Figure 30. Graph of RMSEs as a function of the number of GCPs and off nadir angle, ENVI software, RPC modelling, Pléiades Neo 4

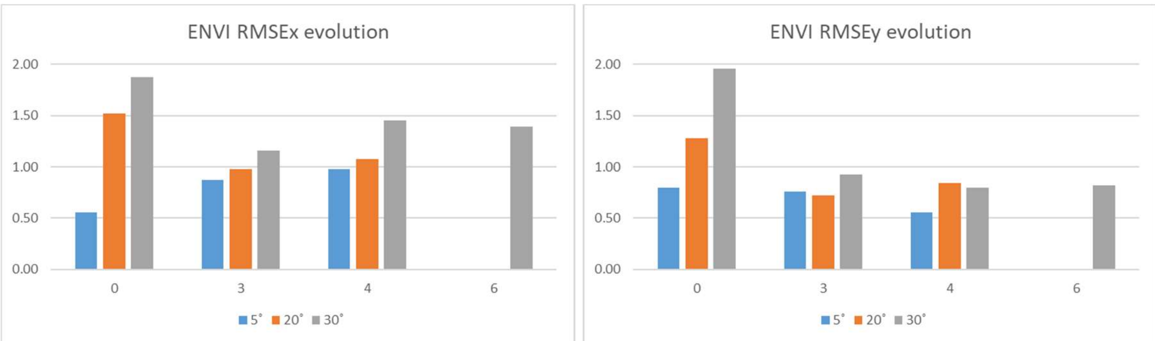

Source: JRC

Figure 31. Graph of RMSEs as a function of the number of GCPs and off nadir angle, ERDAS software, Rigorous modelling, Pléiades Neo 4

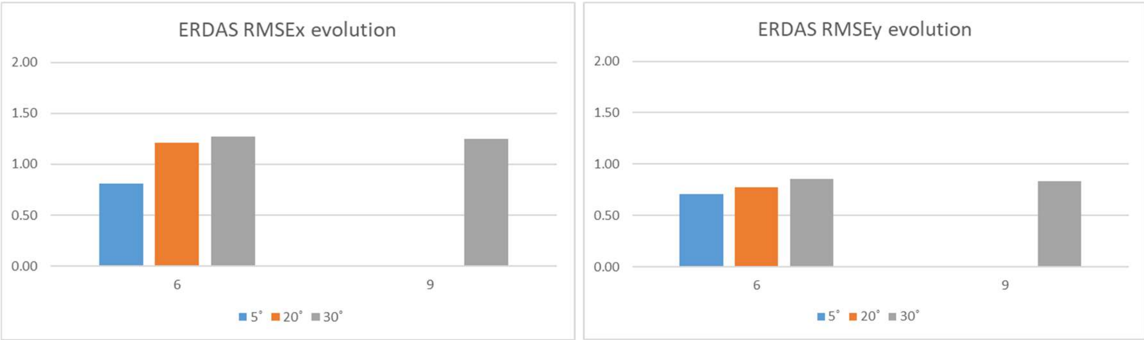

Source: JRC

Figure 32. Graph of RMSEs as a function of the number of GCPs and off nadir angle, ENVI software, Rigorous modelling, Pléiades Neo 4

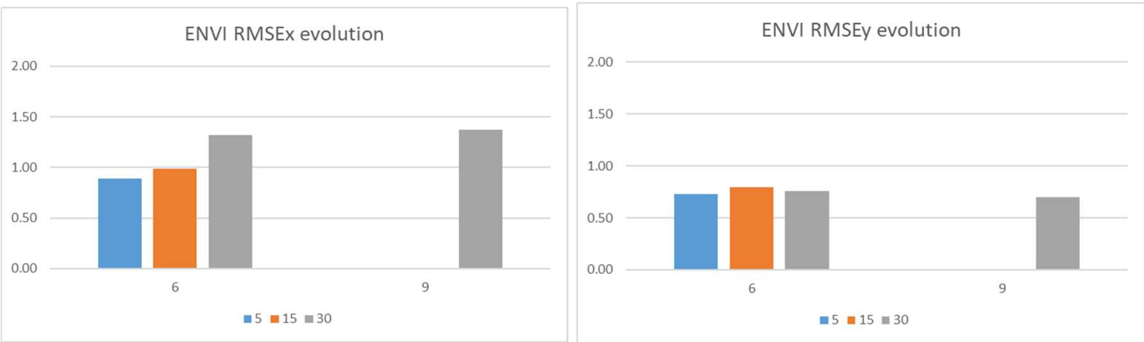

Source: JRC

Comparing the results displayed in ***Figure 25*** to ***Figure 32*** we can draw the following conclusions:

Unsurprisingly, the 1-D RMS errors are sensitive to the off nadir angle of acquisition, the higher the angle, the higher the errors induced.

For both Neo sensors, with 30 deg. ONA, obtained Orthoimages becomes out of requested positional accuracy if no GCPs are used. For PNeo 4 sensor, this is even observed with 20 Deg. ONA;

With RPC modelling, obtained imagery are also out of requested positional accuracy when 30 deg. ONA even if number of GCPs are high;

A systematic bias is observed in the Easting direction (RMSEx) which decreases with the increasing off nadir angle of the acquired image. Reasons for these observed biases have not been further analysed since corresponding RMSEs are within requested specifications.

8.5 Impact of Pleaides sensors

When analysing ***Figure 25*** to ***Figure 32***, one can observe that:

- For Pléiades NEO 4 a bias is observed toward the north direction (RMSEy) that increases with increasing off-nadir nadir angles of the source image.
- Some other differences can be observed between the two sensors depending on the acquisition angles or the number of GCPS used for their ortho rectification. Nevertheless, these differences can be considered as not significant (could be confirmed with more images), thus both sensors can be considered as providing similar ortho products.

8.6 Summarising values

For Pléiades Neo 3 sensor, the obtained results with RPC and more than 3 GCPs used were:

- 5 deg. off Nadir
  - RMSEx = 0.84 m
  - RMSEy = 0.88 m
- 20 deg. off nadir

        - RMSEx = 0.86 m
        - RMSEy = 0.70 m
    - 30deg. off nadir
        - RMSEx = 1.28 m
        - RMSEy = 0.67 m

For Pléiades PNeo 4 sensor the obtained results with RPC and more than 3 GCP used were:

- 5 deg. off nadir
    - RMSEx = 0.77 m
    - RMSEy = 0.70 m
- 20 deg. off nadir
    - RMSEx = 1.05 m
    - RMSEy = 0.83 m
- 30 deg. off nadir
    - RMSEx = 1.20 m
    - RMSEy = 0.83 m

Both software packages Erdas and ENVI perform equally.
These obtained values are all within the requested spatial accuracy to qualify Pléiades Neo VHR data to be used in the frame of the CAP 2014+ direct payments' management.

9 Conclusions

In the light of the benchmark tests performed, both by Airbus and independently by the JRC, on Pléiades NEO ortho products, one can draw the following conclusions:

- On average, the Neo ortho imagery geometric accuracy meets the requirements of RMSEx ≤1.25m and RMSEy ≤1.25 for the VHR prime profiles defined in the VHR profile based technical specifications;
- Consequently, Neo ortho imagery geometric accuracy meets the requirement of 5 m 1D RMSE corresponding to the VHR backup profile defined in the VHR profile based technical specifications.
- These results were obtained for tests with imagery acquired with 5˚, 20˚ and 30˚ Off Nadir Angles, with at least 3 GCPs use for orthorectification and with RPC or rigorous models.
- It must be noted that when rectification were made without GCPs, results obtained become out of specification for acquisitions 30˚ ONA and even 20˚ in some case for Pléiades Neo4 sensor.
- To note also, that at the time of the benchmark analysis, Airbus production chain was not yet fully finalised and internal references were not yet implemented. Airbus recently informed us that, according to the tests they performed using internal references that will be implemented soon in its production chain, the results are within the specifications whatever the PNEO sensor for angles up to 30° ONA. This should be further confirmed but the JRC benchmarking work was already concluded at the time of this notification.

One should note also that, sometimes, atypical results were obtained such as higher RMSE observed for near nadir acquisition compared to 20˚ or 30˚ ONA. However, the number of tested images was insufficient to further investigate this phenomenon.

Finally, one should remind that the available JRC's GCPs dataset is now dating. Several points became unreliable since changes occurred on the ground. Even if these points were generally discarded, one can argue that RMSEs estimated may hold some uncertainty. JRC is conscious of that fact, but since the sensor benchmarking activity was to be stopped with the entry into force of the new CAP (January 2023), the organisation of a new GCP dataset acquisition campaign over Maussane area was not judged imperative.

For the CAP 2023+, new technical specifications will be set to comply with the new VHR imagery use requirements i.e. in the frame of Quality Assessment processes. Should sensor benchmarking tests be put in place, they would need to be done according to these up-dated technical specifications.

References

i. Kapnias, D., Milenov, P., Kay, S. (2008) Guidelines for Best Practice and Quality Checking of Ortho Imagery. Issue 3.0. Ispra

ii. VHR Image Acquisition Specifications for the CAP checks (CwRS and LPIS QA) https://g4cap.jrc.ec.europa.eu/g4cap/Portals/0/Documents/D.3.1%20VHR_Specs_2022_final_new.pdf

iii. Nowak Da Costa, J., Tokarczyk P., 2010. Maussane Test Site Auxiliary Data: Existing Datasets of the Ground Control Points. The pdf file received on 06.02.2014 via FTP.

iv. Lucau, C., Nowak Da Costa J.K. (2009) Maussane GPS field campaign: Methodology and Results. Available at http://publications.jrc.ec.europa.eu/repository/bitstream/111111111/14588/1/pubsy_jrc56280_fmp11259_sci-tech_report_cl_jn_mauss-10-2009.pdf

v. Lucau, C. (2012) Maussane GNSS field campaign 21-26 November 2012

vi. Maussane test site (& geometry benchmarks). KO-Meeting-Presentation January 30, 2014.

vii. Nowak Da Costa, J.K., Walczynska, A. (2011). Geometric Quality Testing of the WorldView-2 Image Data Acquired over the JRC Maussane Test Site using ERDAS LPS, PCI Geomatics and Keystone digital photogrammetry software packages – Initial Findings with ANNEX. Available at http://publications.jrc.ec.europa.eu/repository/bitstream/111111111/22790/1/jrc60424_lb-nb-24525_en-c_print_ver.pdf

viii. Nowak Da Costa, J.K., Walczynska, A. (2010). Geometric Quality Testing of the Kompsat-2 Image Data Acquired over the JRC Maussane Test Site using ERDAS LPS and PCI GEOMATICS remote sensing software. Available at http://publications.jrc.ec.europa.eu/repository/bitstream/111111111/15039/1/lbna24542enn.pdf

ix. Nowak Da Costa, J.K., Walczynska, A., 2010. Evaluating the WorlView-2, GeoEye-1, DMCII, THEOS and KOMPSAT-2 imagery for use in the Common Agricultural Policy Control with Remote Sensing Programme. Scientific presentation at the 16th Conference on ''Geomatics in support of the CAP" in Bergamo, Italy, 24-26 November 2010. JRC Publication Management System.

x. Grazzini, J., Astrand, P., (2013). External quality control of Pléiades orthoimagery. Part II: Geometric testing and validation of a Pléiades-1B orthoproduct covering Maussane test site. Available at http://publications.jrc.ec.europa.eu/repository/handle/JRC83367

xi. Grazzini, J., Lemajic, S., Astrand, P., (2013). External quality control of Pléiades orthoimagery. Part I: Geometric benchmarking and validation of Pléiades-1A orthorectified data acquired over Maussane test site. Available at http://publications.jrc.ec.europa.eu/repository/bitstream/111111111/29541/1/lb-na-26-101-en-n.pdf

xii. Grazzini, J., Astrand, P., (2013). External quality control of SPOT6. Geometric benchmarking over Maussane test site for positional accuracy assessment orthoimagery. Available at http://publications.jrc.ec.europa.eu/repository/bitstream/111111111/29232/1/lb-na-26-103-en-n.pdf

xiii. Blanka Vajsova, B., Walczynska, A., Åstrand, P., Bärisch, S., Hain, S., (2014). New sensors benchmark report on Kompsat-3. Geometric benchmarking over Maussanne test site for CAP purposes. Available at http://publications.jrc.ec.europa.eu/repository/bitstream/JRC93093/lb-na-27064-en-n.pdf

xiv. Blanka Vajsova, B., Walczynska, A., Åstrand, P., Bärisch, S., Hain, S., (2015). New sensors benchmark report on WorldView-3. Geometric benchmarking over Maussane test site for CAP purpose. Available at http://publications.jrc.ec.europa.eu/repository/bitstream/JRC99433/reqno_jrc99433_lb-na-27673-en-n.pdf

xv. https://www.l3harrisgeospatial.com/Software-Technology/ENVI

xvi. https://hexagon.com/products/erdas-imagine

List of abbreviations and definitions

ADS40	Airborne Digital Sensor 40
AOI	Area of Interest
CAP	Common Agricultural Policy
CE90	Circular Error 90%
CwRS	Control with Remote Sensing
DEM	Digital Elevation Model
EQC	External Quality Control
EUSI	European Space Imaging
GCP	Ground Control Point
GIS	Geographic Information System
GNSS	Global Navigation Satellite System
GPS	Global Positioning System
GSD	Ground Sample Distance
ICP	Independent Check Point
IQC	Internal Quality Control
IR	Infrared
JRC	Joint Research Centre
NED	Near Infrared, Red Edge, Deep Blue
NIR	Near-infrared
ONA	Off-Nadir Angle
PAN	Panchromatic
QC	Quality Check
RGB	Red, Green, Blue
RMSE	Root Mean Square Error
RPC	Rational Polynomial Coefficients
STRM	Shuttle Radar Topography Mission
UTM	Universal Transverse Mercator
VHR	Very High Resolution
VNIR	Visible and Near-InfraRed
WGS84	World Geodetic System '84
PNeo	Pléiades Neo
1-D	One-dimensional

List of figures

Figure 1. Location of the test site and its AOI 9

Figure 2. Distribution of GCPs available in the AOI, the background image is an elevation map of the area.. 11

Figure 3. Distribution of 9 GCPs selected for orthorectification process, the background image represents an elevation map of the area and the red square corresponding to the study AOI. 12

Figure 4. Distribution of 9 GCPs selected for internal control, the background image represents an elevation map of the area and the red square corresponding to the study AOI 13

Figure 5. Relief of the study AOI 14

Figure 6. Interface OneAtlas with order parameters 16

Figure 7. View in natural colour (RGB) and false colour (NED) of one acquired scene 17

Figure 8. Standard benchmarking procedure 19

Figure 9. RMSEx and RMSEy depending on the sensor 22

Figure 10. RMSEx and RMSEy depending on the acquisition angle 23

Figure 11. RMSEx and RMSEy depending on the orthorectification model used 23

Figure 12. RMSEx and RMSEy depending on the number of GCPs used 24

Figure 13. RMSEx and RMSEy depending on the number of GCPs used 24

Figure 14. ICPs dataset used by JRC in the EQC of PNeo ortho imagery. 27

Figure 15. Point representation of planimetric RMSE 1D errors calculated on ortho images using JRC ICPs dataset for PNeo3 32

Figure 16. Point representation of planimetric RMSE 1D errors calculated on ortho images using JRC ICPs dataset – PNeo4 32

Figure 17. Behaviour of RMSEs across the various number of GCPs for ERDAS and ENVI software, source image 5˚off nadir – PNeo3, RPC modelling 33

Figure 18. Behaviour of RMSEs across the various number of GCPs for ERDAS and ENVI software, source image 5˚off nadir – PNeo4, RPC modelling 33

Figure 19. Behaviour of RMSEs across the various number of GCPs for ERDAS and ENVI software, source image 20˚off nadir – PNeo3, RPC modelling 34

Figure 20. Behaviour of RMSEs across the various number of GCPs for ERDAS and ENVI software, source image 20˚off nadir – PNeo4, RPC modelling 34

Figure 21. Behaviour of RMSEs across the various number of GCPs for ERDAS and ENVI software, source image 30˚off nadir – PNeo3, RPC modelling 34

Figure 22. Behaviour of RMSEs across the various number of GCPs for ERDAS and ENVI software, source image 30˚off nadir – PNeo4, RPC modelling 35

Figure 23. Behaviour of RMSEs across the various number of GCPs for ERDAS and ENVI software, source image 30˚off nadir – PNeo3, Rigorous modelling 35

Figure 24. Behaviour of RMSEs across the various number of GCPs for ERDAS and ENVI software, source image 30˚off nadir – PNeo4, Rigorous modelling 36

Figure 25. Graph of RMSEs as a function of the number of GCPs and off nadir angle, ERDAS software, RPC modelling, Pléiades Neo 3 37

Figure 26. Graph of RMSEs as a function of the number of GCPs and off nadir angle, ENVI software, RPC modelling, Pléiades Neo 3 37

Figure 27. Graph of RMSEs as a function of the number of GCPs and off nadir angle, ERDAS software, Rigorous modelling, Pléiades Neo 3 37

Figure 28. Graph of RMSEs as a function of the number of GCPs and off nadir angle, ENVI software, Rigorous modelling, Pléiades Neo 3 38

Figure 29. Graph of RMSEs as a function of the number of GCPs and off nadir angle, ERDAS software, RPC modelling, Pléiades Neo 4 38

Figure 30. Graph of RMSEs as a function of the number of GCPs and off nadir angle, ENVI software, RPC modelling, Pléiades Neo 4 38

Figure 31. Graph of RMSEs as a function of the number of GCPs and off nadir angle, ERDAS software, Rigorous modelling, Pléiades Neo 4 38

Figure 32. Graph of RMSEs as a function of the number of GCPs and off nadir angle, ENVI software, Rigorous modelling, Pléiades Neo 4 39

List of tables

Table 1. General characteristics of the Pléiades Neo constellation ... 4

Table 2. Orbital characteristics and viewing capability ... 4

Table 3. Key attributes of the Pléiades Neo Constellation ... 5

Table 4. Standard product options delivered by Image Production Facility ... 6

Table 5. Ground Control Points available for the Maussane test site ... 10

Table 6. Collection used for the 9 GCPs selected for the orthorectification process ... 11

Table 7. Collection used for the 9 GCPs selected for the internal control ... 12

Table 8. ORI and CORI accuracy specifications ... 15

Table 9. DTM vertical accuracy specifications ... 15

Table 10. Aerial Orthomosaics Specifications ... 15

Table 11. Real angles of the primary product across study AOI ... 16

Table 12. Tested Scenarios ... 19

Table 13. Distribution of tests according to parameters ... 21

Table 14. Acquired Images ... 22

Table 15. Identical check points specifications ... 26

Table 16. ICPs overview ... 27

Table 17. Obtained quality control results (RMSE1D) on ortho image produced by applying Rational Function Modelling, using JRC ICPs dataset – PNeo3 ... 30

Table 18. Obtained quality control results (RMSE1D) on ortho image produced by applying Rational Function Modelling, using JRC ICPs dataset – PNeo4 ... 30

Table 19. Obtained quality control results (RMSE1D) on ortho image produced by applying Rigorous Modelling, using JRC ICPs dataset – PNeo3 ... 31

Table 20. Obtained quality control results (RMSE1D) on ortho image produced by applying Rigorous Modelling, using JRC ICPs dataset – PNeo4 ... 31

Table 21. Obtained quality control results (RMSE1D) on ortho images produced by applying Airbus automatic chain, using JRC ICPs dataset – PNEO 3 and PNEO 4 ... 36

Science for policy

The Joint Research Centre (JRC) provides independent, evidence-based knowledge and science, supporting EU policies to positively impact society

EU Science Hub
joint-research-centre.ec.europa.eu

@EU_ScienceHub

EU Science Hub - Joint Research Centre

EU Science, Research and Innovation

EU Science Hub

@eu_science

Publications Office
of the European Union